Asian Journal of Pharmaceutical Sciences 15 (2020) 416–448

Available online at www.sciencedirect.com

ScienceDirect

journal homepage: www.elsevier.com/locate/AJPS

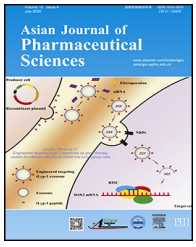

Review

Tumor microenvironment responsive drug delivery systems

Qunye He[a,1], *Jun Chen*[a,1], *Jianhua Yan*[a], *Shundong Cai*[a], *Hongjie Xiong*[a], *Yanfei Liu*[c], *Dongming Peng*[d], *Miao Mo*[b,*], *Zhenbao Liu*[a,*]

[a] *Xiangya School of Pharmaceutical Sciences, Central South University, Changsha 410013, China*
[b] *Department of Urology, Xiangya Hospital, Central South University, Changsha 410008, China*
[c] *School of Chemistry and Chemical Engineering, Central South University, Changsha 410083, China*
[d] *School of Pharmacy, Hunan University of Chinese Medicine, Changsha 410208, China*

ARTICLE INFO

Article history:
Received 29 April 2019
Revised 30 July 2019
Accepted 21 August 2019
Available online 26 September 2019

Keywords:
Cancer therapy
Stimuli responsive
Dynamic targeting
Drug delivery system
Controlled release

ABSTRACT

Conventional tumor-targeted drug delivery systems (DDSs) face challenges, such as unsatisfied systemic circulation, low targeting efficiency, poor tumoral penetration, and uncontrolled drug release. Recently, tumor cellular molecules-triggered DDSs have aroused great interests in addressing such dilemmas. With the introduction of several additional functionalities, the properties of these smart DDSs including size, surface charge and ligand exposure can response to different tumor microenvironments for a more efficient tumor targeting, and eventually achieve desired drug release for an optimized therapeutic efficiency. This review highlights the recent research progresses on smart tumor environment responsive drug delivery systems for targeted drug delivery. Dynamic targeting strategies and functional moieties sensitive to a variety of tumor cellular stimuli, including pH, glutathione, adenosine-triphosphate, reactive oxygen species, enzyme and inflammatory factors are summarized. Special emphasis of this review is placed on their responsive mechanisms, drug loading models, drawbacks and merits. Several typical multi-stimuli responsive DDSs are listed. And the main challenges and potential future development are discussed.

1. Introduction

Tumor microenvironment responsive drug delivery systems are “smart” formulations exhibiting an on-demand drug release profile upon response to stimulations from tumor cellular environments, which have aroused great interests in the nano-medical field. Through shrinking or expanding in size, changing of the surface charge, or regulation of

* Corresponding authors. Central South University, No. 172, Tongzipo Road, Changsha 410013, China. Tel.: +86 13723886533.
E-mail addresses: docmon@csu.edu.cn (M. Mo), zhenbaoliu@csu.edu.cn (Z.B. Liu).
[1] These authors contributed equally to this work.
Peer review under responsibility of Shenyang Pharmaceutical University.

https://doi.org/10.1016/j.ajps.2019.08.003

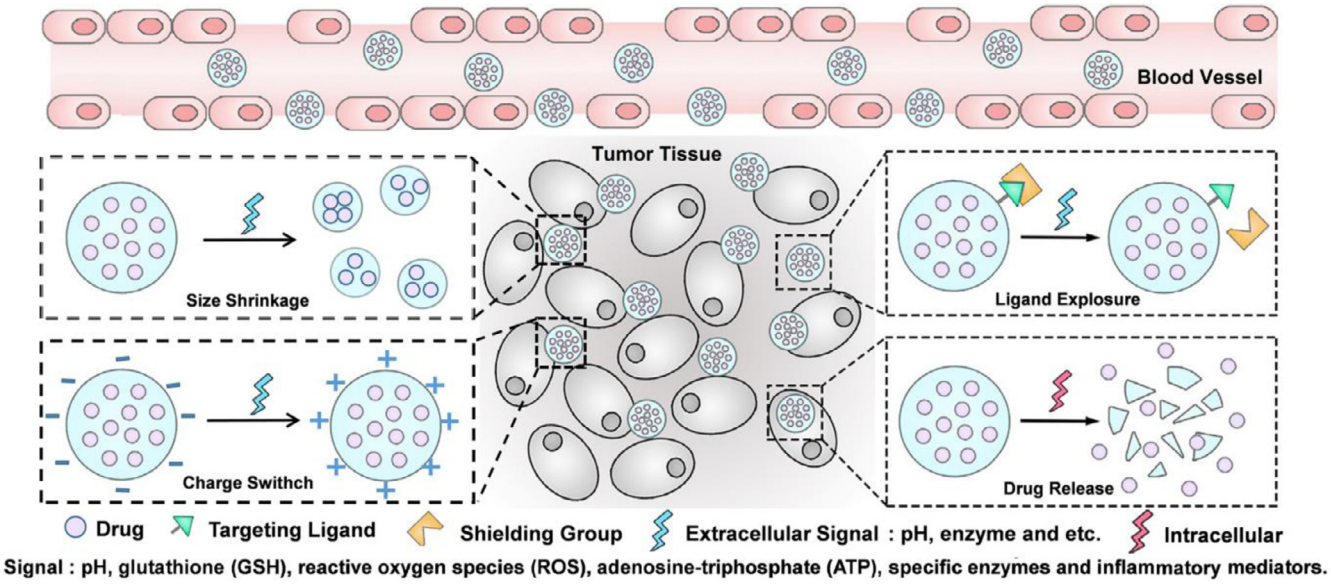

Fig. 1 – Tumor microenvironment-activatable targeting and self-controlled drug release (Reproduced with permission from [9]. Copyright 2016 The Authors).

other physiochemical properties, tumor stimuli-responsive drug delivery could be achieved [1]. Traditional targeting strategies including passive and active targeting face many challenges. For passive target, the enhanced permeability and retention effects (EPR) are involved, however, EPR effects require the diameter of the nanocarriers larger than 100 nm, but tumor penetration favors the size around 30 nm, which means that nanocarriers with desired EPR effects cannot exhibit favorable tumor penetration. For active targeting, target ligands are utilized to recognize cellular overexpressed receptors [2], however, the ligands have non-specific interaction with plasma protein or normal cells during blood circulation. Compared with conventional nanocarriers, stimuli-responsive drug delivery systems employ the conjugation of stimuli responsive moieties onto the nanocarriers for property alterations, such as size shrinkage, surface charge switch and ligand hidden or exposure, thus to ensure that the nanocarriers have the needed properties for efficient tissue accumulation, penetration, cellular endocytosis and drug release. These smart DDSs exhibit excellent superiorities on enhanced therapeutic effects and reduced side effects, thus holding tremendous potential in the targeted delivery of therapeutic agents.

The design rationale of these DDSs is based on the using of physiochemical distinctions between cancer and normal cells to introduce functional groups responding to different stimuli onto nano-carriers, which endows them with desired response to different tumor associated signals. Tumor microenvironment-sensing moieties could be modified via physical absorption [3] or chemical reaction [4]. Bond cleavage, disassembly or cap removal are usually employed to promote drug release at the desired site. Based on rational design, combination of several functional moieties within a single carrier to fabricate multi-stimuli responsive nanocarriers could achieve specific targeting, on-demand drug release (Fig. 1), and even more sophisticated drug delivery.

Multi-stimuli responsive nanocarriers exhibit smart behaviors at biological environments [5]. It is commonly accepted that intravenously administered nano-formulations usually go through a cascade of five steps, which include blood circulation (C), tumor accumulation (A), deep tumor tissue penetration (P), cellular internalization (I) and intracellular drug release (R): for short is CAPIR cascade (Fig. 2) [7]. Each step requires specific nano-properties, which can be summarized as the "3S" transition requirements [7]. The DDSs should be "stable" enough to hold the drugs tightly on the way to cancer cells, while drugs should be released rapidly upon internalization [7]. The "surface" properties of DDSs should be hydrophilic coated (*e.g.* PEGylated) and neutral charged for prolonged circulation time, and the targeting ligands (*e.g.* folic acid) should be shielded during the systemic circulation, while at the tumor site, the ligands should be unshielded to facilitate the binding between ligands with cell-membrane receptors and fulfill the cellular internalization [7,8]. The "size" should be around 100 nm for effective accumulation, but be smaller than 30 nm for deep tumor penetration [7]. Successive modification of various stimuli sensitive functionalities onto a single carrier can induce a more prominent or more refined response of the carriers toward different tumor associated stimuli. Thus, rational combination of several responsive groups will make it possible to design a multi-functional carrier, which can rapidly perceive and respond to one or more tumor micro-environmental signals, exhibiting "real time" transition of physiochemical properties and self-controlled drug release at the specific location with a precise concentration.

Some stimuli-sensitive functional moieties modified drug delivery systems have been reported recently [9–11], while systematic and detailed reviews on these DDSs are rare. Specially, Chen et al. reviewed the polymer-based platinum DDSs where the drug can be activated either by intracellular GSH, ascorbic acid or ultraviolet light [10]. Huang et al. discussed the application of stimuli responsive

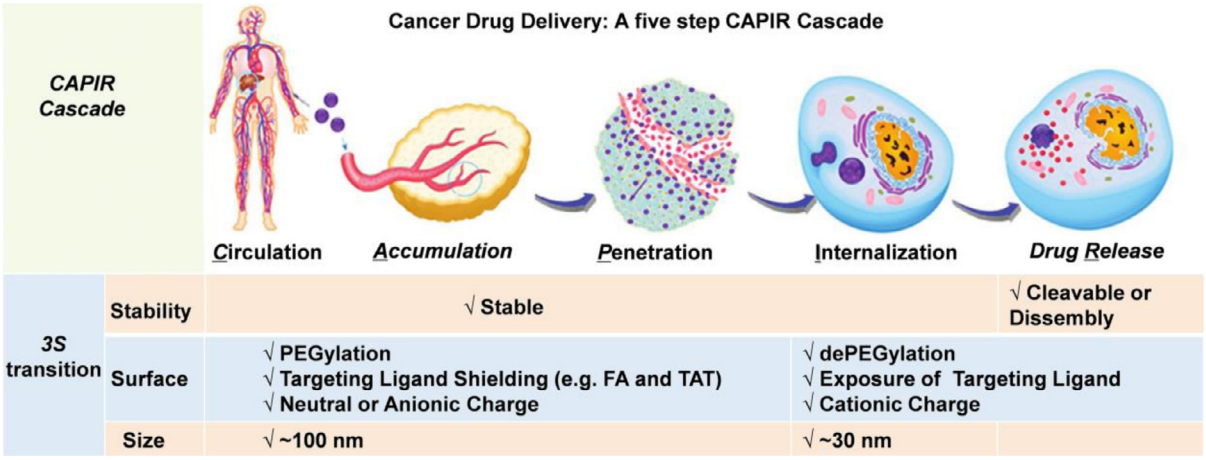

Fig. 2 – Summary of the 3S transitions in the CAPIR cascade for a nano-formulation to achieve optimal drug-delivery (Reproduced with permission from [6]. Copyright 2017 Wiley-VCH.).

Table 1 – Physiochemical distinctions between some common tumor and normal tissues.

Physiochemical signals	Normal tissues	Tumor tissues	Tumor models	References
pH	7.4 (human plasma)	~6.8 in tumor extracellular environment	H9618a cells	[204]
		4.3–5.2 in the endosomes and lysosomes	U937 cells	[48]
GSH	~140 nmol/g tissue	~90 nmol/g tissue (extracellular)	Breast solid tumors	[205]
		1–10 μM (intracellular)	HeLa cells	[206]
ROS	~3 μM (human plasma)	50–100 μM (extracellular)	HeLa cells	[109,115,207]
ATP	<5 μM (human plasma)	< 0.4 mM (extracellular)	Leukemia, lymphoma, neuroblastoma cells of mouse and hepatoma cells of rat	[129,208–210]
		1–10 mM (intracellular)	Leukemia, lymphoma, neuroblastoma cells of mouse and hepatoma cells of rat	[129]
Enzyme	Low expression	Upregulation in the cellular compartments	Human breast cancer	[159]
Inflammatory mediators	Low expression (normal tissue)	Overexpression in tumor tissues	Colorectal carcinoma, lung carcinoma, and bladder carcinoma, etc.	[180]

bio-based polymers in drug delivery [11]. They focused on both endogenous and exogenous stimuli, such as pH, light, ultrasound, mechanical forces, electric field and magnetic field. Gu et al. described the design strategies of novel nanoscale materials responsive to various intracellular signals [9]. However, a comprehensive summary of the targeting strategies and tumor responsive functional moieties, as well as the multi-stimuli responsive DDSs are lacked. Here, we systematically reviewed the progresses made in tumor microenvironment responsive drug delivery systems. Special emphasis is put on tumor targeting strategies and stimuli-responsive functionalities. Three dynamic targeting strategies are summarized, including size shrinkage, surface charge conversion and ligand exposure. Functional moieties responding to stimuli, such as pH, glutathione (GSH), reactive oxygen species (ROS), adenosine-triphosphate (ATP), specific enzymes and inflammatory mediators are listed in Table 1. Their sensitive moieties, drug loading models, and responsive mechanisms are mainly discussed. Several typical examples of multi-stimuli responsive DDSs are listed, in which, the tumor associated signals not only trigger the release of the drugs, but also induce physicochemical property transitions of DDSs for more efficient tumor targeting. The main challenges of these smart DDSs and their potential future developments are discussed.

2. Dynamic tumor targeting strategies

Dynamic tumor targeting strategies mean that the slippery carriers are capable of changing their properties for eventually precise drug release. Conventional targeting strategies usually bear unsatisfied systemic circulation time, low-specific tumor targeting and poor penetration into intra-tumoral region partially because of their inferior flexibility and unsatisfied nano-properties [12]. To achieve high efficiency of drug delivery, specific features of nanoparticles are required for adaption to diverse biological environments. In blood circulation, physicochemical characteristics including size and surface chemistry are tailored for long circulation. At tumor tissues, in response to extracellular signals (*e.g.* acidic pH, and overexpressed enzymes), rapid drug release can

be achieved. The release mechanisms, such as protonation, disassembly or bonds cleavage, endow DDSs with on-demand changing of properties, such as smaller size, positive charge, as well as the exposure of the protected ligands for favorable cellular internalization [13].

2.1. Size shrinkage targeting

Nanoscale size is the foundation of passive targeting. To realize efficient drug release, DDSs should accumulate around leaky blood vessels based on EPR effects, then diffuse into deep tumor tissue for cellular uptake [13]. Researches demonstrated that nanoparticles (NPs) with diameter around 100 nm were able to achieve prolonged circulation time and effectively accumulate in tumor tissues [14,15], whereas NPs with diameter smaller than 30 nm exhibited enhanced tumor penetration attributed to their reduced diffusional hindrance [16,17]. This means that NPs with a larger diameter exert excellent EPR effects but low uptake ratio. Size shrinkage targeting is expected to solve such dilemma. For this strategy, various NPs with smaller size are integrated into larger nanoparticles via encapsulation or surface conjugation. The initial size of the platform is around 100 nm for satisfactory circulation and accumulation. Subsequently, tumor extracellular stimuli enables the shrinkage of the NPs to form a smaller size for deep tumor penetration. Han et al. employed poly (amidoamine) (PAMAM) dendrimers as the core, onto which, hyaluronic acids (HA) were attached via metalloproteinase-2 (MMP-2) cleavable peptides, forming larger particles which can undergo a size reduction from 200 to 10 nm in response to extracellular MMP-2 [18]. Wang et al. designed raspberry-like NPs with size transition from 104 to 5 nm at acidic tumor microenvironment [19]. The NPs were co-assembled into a raspberry-like structure (iCluster/Pt) using poly (ethylene glycol)-b-poly (ε-caprolactone) (PEG-b-PCL) and PAMAM-graft-polycaprolactone, and platinum (Pt) prodrugs were attached through acid responsive amide bonds (PCL-CDM-PAMAM/Pt). Furthermore, the PAMAM/Pt dendrimers with a size of 5 nm could be detached from the surface of the NPs in response to acidic environment (pH 6.8). Such a sharp size change could promote both enhanced tumor accumulation and efficient tumor penetration (Fig. 3A). Size shrinkage was also reported to combine with collagen depletion strategy for deep intra-tumoral penetration [20]. In this case, size shrinkable gold nanoparticles loaded with DOX (DOX-AuNPs) were embedded or adhered onto MMP-2 degradable gelatin NPs (DOX-AuNPs-GNPs) which can shrink from 117.8 nm to less than 50 nm at MMP-2 overexpressed tumor extracellular matrix (ECM). Combined pretreatment with a collagen depletion agent (losartan) enabled the digestion of the collagen network in tumor ECM and broke down interstitial stromal barriers, thus the shrinkable DOX-AuNPs-GNPs exhibited striking penetration and excellent drug delivery profile in collagen expressing 4T1 breast tumors.

2.2. Surface charge switchable targeting

Surface charge plays a vital role in passive targeting. Carriers with negative or neutral charge often possess prolonged circulation time and relatively high accumulation in tumor tissues, which attribute to avoidance of recognition and subsequent elimination from opsonization and mononuclear phagocytic systems (MPSs) [21]. In contrast, cationic NPs are able to obtain an improved cellular internalization via electrostatic interactions with anionic cancer cell membranes [22], as well as promote endosomal escape based on "proton sponge" effect to avoid drug degradation in lysosomes [23,24]. That's the charge contradiction of NPs. Protein corona effect is a result of this contradiction where electrostatic interactions promote the covering of blood proteins on the surface of nanocarriers, resulting in non-specific cellular internalization. To address this issue, NPs with switchable surface charge have been developed. Initially, the NPs bear negative or neutral charge to hide from nonspecific adsorption from normal cells or plasma proteins. After arriving at tumor parenchyma, tumor extracellular signals, generally the acidic signal ($pH_e \approx 6.8$), triggered their surface charge conversion into a positive one, thus to promote the interaction of the NPs with the anionic membrane of cancer cells (Fig. 3B) [25]. The frequently reported pH_e liable moieties are 2-propionic-3-methylmaleic anhydride (CDM) and 2, 3-dimethylmaleic amide (DMMA), both of which are attached onto amino terminated polymers forming acidic responsive amide linkers. Sun et al. reported a pH_e responsive micelleplex by attaching PEG-CDM onto amino modified poly-DL-lactide (PDLLA) [26]. The obtained copolymers showed acidic (pH 6.5) responsive detachment of PEG layer and considerate increase of zeta potential, thus contributing to efficient NPs cellular internalization and chemotherapeutic delivery. Besides, they synthesized another similar copolymer composed of a CDM-modified PEG corona, an amide linker and siRNA conjugates with anionic cell penetrating peptide (CPPs) [27]. Upon tumor accumulation, the amide linkers of the copolymer were cleaved in response to acidic signals (pHe = 6.5), leading to the detachment of the PEG corona. This accompanied with the exposure of the cationic CPPs to facilitate cellular internalization and efficient nuclei-targeted delivery of siRNA. DMMA was also applied to the development of the pH_e liable materials. Feng et al. developed DMMA coated carbon dots (CDs) for enhanced cisplatin (Pt (IV)) delivery [28,29]. Anionic PEG-(PAH/DMMA) polymers served as the shell for hiding the cationic Pt (IV) loaded CDs from the blood serum. Mild acidic (pHe = 6.8) at tumor extracellular matrix (ECM) facilitated the hydrolysis of the amide bonds between PEG-PAH and DMMA, and thus endowed the resulted polymers with positive charge, which led to the electrostatic repulsion between the CDs core and the polymer shell. This is also accompanied with polar transition of the polymer from hydrophilic to hydrophobic, resulting in shell dissociation and further exposure of the positive charged CDs-Pt (IV). In addition to PEG corona, He's group reported a novel strategy to avoid nonspecific absorption from plasma proteins [30–32]. In their works, the model drug was linked with maleimide via tumor responsive moieties to form the prodrug. And via the maleimide groups, the prodrugs were pre-incubated with albumin before administration. Due to the fact that the binding sites of the prodrugs for plasma proteins have been saturated with albumin, thus nonspecific interaction was largely decreased. When arriving at tumor tissue, the sensitive linkers were degraded, resulting in the detachment of the albumin and efficient release of the model drugs.

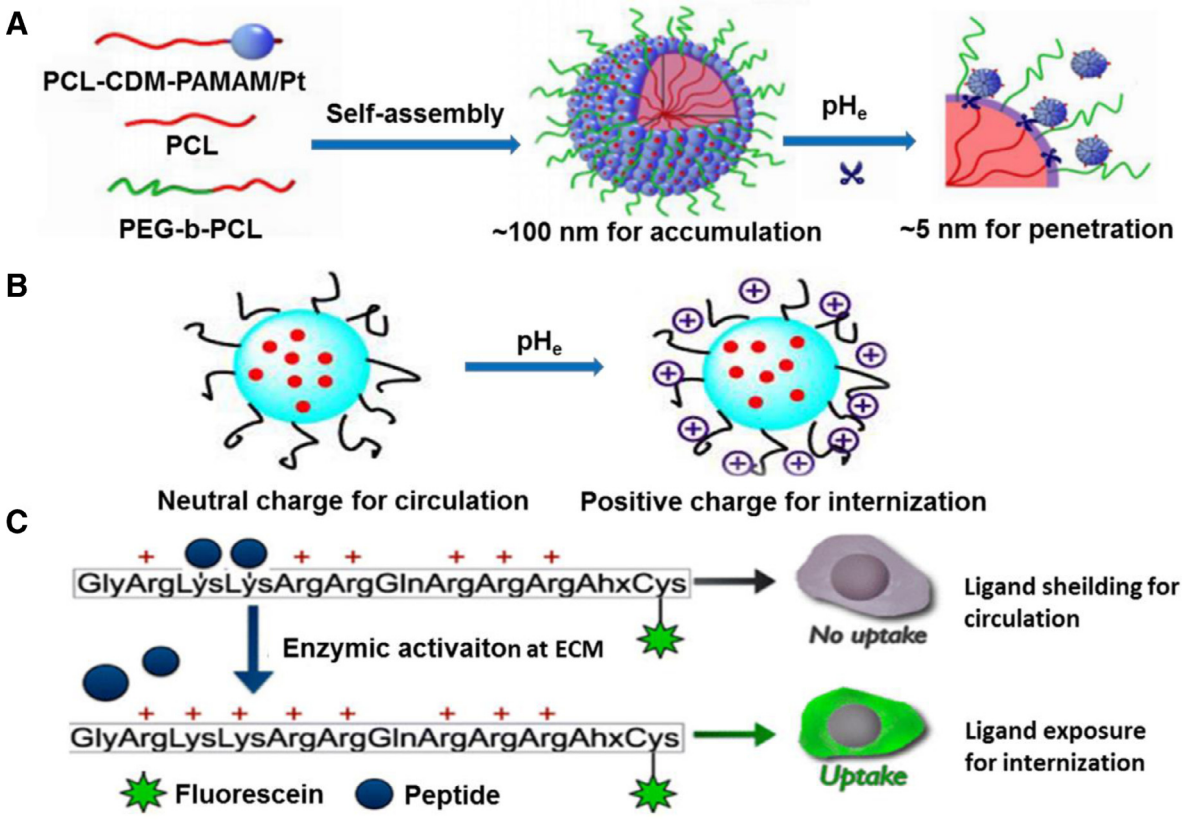

Fig. 3 – Dynamic targeting strategies for enhanced drug delivery. (A) Size shrinkage targeting (Reproduced with permission from reference [19]. Copyright 2016 National Academy of Sciences); (B) Surface charge conversion targeting (Reproduced with permission from [25]. Copyright 2016 Ivyspring) (C) TAT CPPs targeting ligand exposure strategy (Reproduced with permission from [42]. Copyright 2015, American Chemical Society).

2.3. *Surface ligand activatable targeting*

Tumor active targeting, another landmark discovery in anticancer drug delivery, involves the use of specific ligands attached onto the surface of nanoscale carriers. The strategy is expected to realize selective recognition of appropriate receptors or antigens overexpressed by cancer cells or tumor vasculature, thus promoting the cellular uptake of the loaded cargo via receptor-mediated endocytosis. Numerous moieties targeting to tumor cells have been exploited in DDSs design, such as proteins (transferrin) [29], vitamins (FA) [33], peptides (arginine-glycine-aspartic acid and AG73 peptide) [34], nucleic acids (aptamer) [35–37], and some other molecules (hyaluronic acid) [38]. Some moieties allowing specific mitochondria targeting are also developed including triphenylphosphonium, dequalinium, mitochondrial penetrating peptides and mitochondrial protein import machinery [39]. However, many challenges limit the practical application of conventional active targeting strategies. For example, in addition to the pathologic tissues, most receptors are also expressed with low levels in healthy tissues. During systemic circulation, these ligands exhibit strong binding affinity with their original unsaturated receptors on normal tissues, especially the reticuloendothelial system (RES), which causes undesired high NPs accumulation in healthy tissues. Therefore, smart ligand targeting strategies are designed to address such problems. Usually, targeting ligands are shielded from nonspecific interaction with non-cancerous cells during systemic circulation. Subsequently, the targeting moieties will be emerged and become effective after locating at tumor sites for enhanced tumor cellular internalization.

Take cell penetrating peptides (CPPs) as an example. CPPs are positively charged short peptides which are able to facilitate cellular intake/uptake of various substances, including small chemical molecules, bio-macromolecules, and NPs. Their targeting ability generally comes from the interactions between amino acid residues and specific receptors [40]. Substitution of these functional moieties with stimuli responsive bonds or groups will decrease their targeting capacity and even make them inactive, for example, amino acids with acidic responsiveness [41] or peptides with enzyme responsiveness (Fig. 3C) [42,43]. In a study by Liu et al., legumain protease upregulating in diverse types of tumor tissues was applied as triggers to activate the transmembrane transport capacity of CPPs (TAT, trans-activating transcriptional activator) [43]. In their work, alanine-alanine-asparagine (AAN) peptide, a substrate of legumain protease, was attached to the fourth lysine of the cell penetrating peptides with activity blocked by 72.65%. At

tumor microenvironment, once the AAN linker was removed by the overexpressed legumain protease, the hidden TAT peptides were exposed and led to effective recovery of the internalization capacity. Coating the ligand targeting NPs with sheddable neutral or negative polymers can also block the nonspecific interactions [44,45]. Wang et al. reported an acidity triggered ligand modified NPs where acidic sheddable PEG-PHMA chains served as the shell coating on the surface of the iRGD-modified polymeric prodrug cores [45]. PHMA is the abbreviation of poly (2-(hexamethyleneimino) ethyl methacrylate). The PEG-PHMA shell with a pK_a value of 6.9 underwent amphiphilic to hydrophilic transition because of its protonation at tumor ECM ($pH_e \approx 6.8$). Thus, the PEG-PHMA shields were dissociated from the core, leading to fast activation of the iRGD and enhanced cellular uptake of the prodrug.

3. Stimuli triggered drug delivery

3.1. *pH-triggered drug delivery systems*

Vigorous metabolism in tumor tissues promotes the glucose consumption and lactic acid accumulation, and therefore the pH conditions in tumor tissues are frequently 0.5–1.0 units lower compared with healthy tissues [46,47]. Researches revealed that the pH values of tumor tissue range from 6.5 to 7.2, while for normal tissue the values are around 7.4 [48]. The pH gradients are also found at some intracellular organelles, such as the endosomes and lysosomes, in which the pH is in the range of 4.5–5.5 [48]. Different tumor tissues exhibit different pH values. In an early study, it's confirmed that the pH_e value for adenocarcinoma and soft tissue sarcoma was 6.94 ± 0.08 compared with 7.20 ± 0.07 in squamous cell carcinomas and malignant melanomas lesions [49]. Thus, adenocarcinoma and soft tissue sarcoma might be more responsive to pH-triggered drug delivery systems. This can also explain the reason why most reported DDSs with pH responsiveness utilized adenocarcinoma cells such as MCF-7 cells [50,51], HeLa cells [52,53], and BxPC-3 cells [54] as models to investigate the curative effect. The existing pH differences have received wide application in "size shrinkage" for enhanced tumor penetration, "surface charge conversion" for improved cellular internalization and "stability change" for on-demand drug release at cellular or subcellular level. For example, functional moieties undergo bond cleavage to release smaller size NPs or capture of protons to form a cationic surface at pH_e. Based on the reported acidic sensitive platforms, their responsive mechanisms mainly exist in three forms: bond cleavage, protonation and gas generation.

3.1.1. *pH responsive chemical bonds cleavage*

Bond cleavage is a common mechanism for acid responsive DDSs. In these systems, drugs can be attached to materials through acid labile linkers or encapsulated into the acid labile carriers. So far, various acid labile moieties have been reported such as hydrazine [55], acetal [56], imines [57] and coordination metal-organic frameworks (MOFs) [58]. These linkers are expected to be stable at physiological pH (~7.4) and undergo hydrolyzation at acidic environments (pH 4.5–6.5). Thus, the drug release at specific acidic tumor site can be achieved. Organic linkers were widely reported in numerous reviews [59]. Here, we mainly focused on the metal-organic complexes.

MOFs are metal-organic complexes where organic ligands are bridged to metal ions via coordination bonds, presenting one-, two-, or three-dimensional structures. Zeolitic imidazolate framework-8 (ZIF-8) is one of the most popular MOF materials due to their acceptable biocompatibility. Coordination bonds with acid triggered breakage are key composites of these materials. Tsung's group developed a novel method for the preparation of the acidic responsive ZIF-8 nanospheres where fluorescein was encapsulated within the nanospheres during synthesis (Fig. 4A) [58]. The obtained ZIF-8 nanospheres maintained their size and shape at pH 7.4. After 1 h treatment with acidic buffer (pH 6.0), 50% of the encapsulated fluorescein was released. In addition, the encapsulation of other molecules such as camptothecin (CPT) and iron oxide NPs were also investigated in this study, indicating great versatility of the developed ZIF-8 scaffold. In another study by Zou's group, they reported a one-pot synthesis method for therapeutic agent encapsulation in MOFs [60]. They coordinated therapeutic molecules with different functional groups like carboxyl group with Zn^{2+} ions to facilitate the initial self-assembly of MOFs. And then another different organic linker was further introduced for disassembly of the initial MOFs to form another more stable coordination structure where the therapeutic agents were encapsulated. More than 95% of the doxorubicin (DOX) was released during 7–9 d at acidic environments (pH 5.0–6.0).

In 2016, Kim et al. developed an acid-sensitive mussel adhesive protein (MAP)-based formulation for DOX delivery (Fig. 4B) [61]. In this system, coordination between iron (III) and 3, 4-dihydroxyphenylalanine (DOPA) were served as pH responsive moieties, which triggered drug release at pH 6.0. Sun et al. reported a yolk-like Fe_3O_4@Gd_2O_3 nanoplatform for acid responsive T_1-T_2 dual-mode magnetic resonance imaging (MRI) and cisplatin delivery [62]. Their pH responsiveness was based on the coordination between platinum and amino group on Fe_3O_4@Gd_2O_3 surface. For prolonged circulation and active targeting, PEG and FA were also modified. It was demonstrated that the platform exhibited efficient drug release profile and T_1-T_2 dual-mode MRI at pH 4.5.

3.1.2. *pH responsive protonated chemical groups*

"Protonated" chemical groups, such as carboxylic acid and amine group, can be introduced to materials for pH responsive drug delivery. These groups, with different chemical structures and pKa values, can accept or donate protons and undergo pH-dependent conformational changes, thus leading to on-demand drug release. According to their chemical structure, the reported acidic responsive materials based on pronation can be divided into three types: polymers, biomolecules and inorganic materials.

Based on the charge status at pH 7.4, polymers with acidic responsiveness are classified as anionic polymers and cationic polymers. Kozlovskaya et al. reported acidic responsive erythrocyte-mimicking hydrogel capsules containing anionic poly (methacrylic acid) (PMAA), the pKa of which is around 4.8 [63]. The obtained capsules exhibited a controlled shape transition related to pH-regulated volume change, which

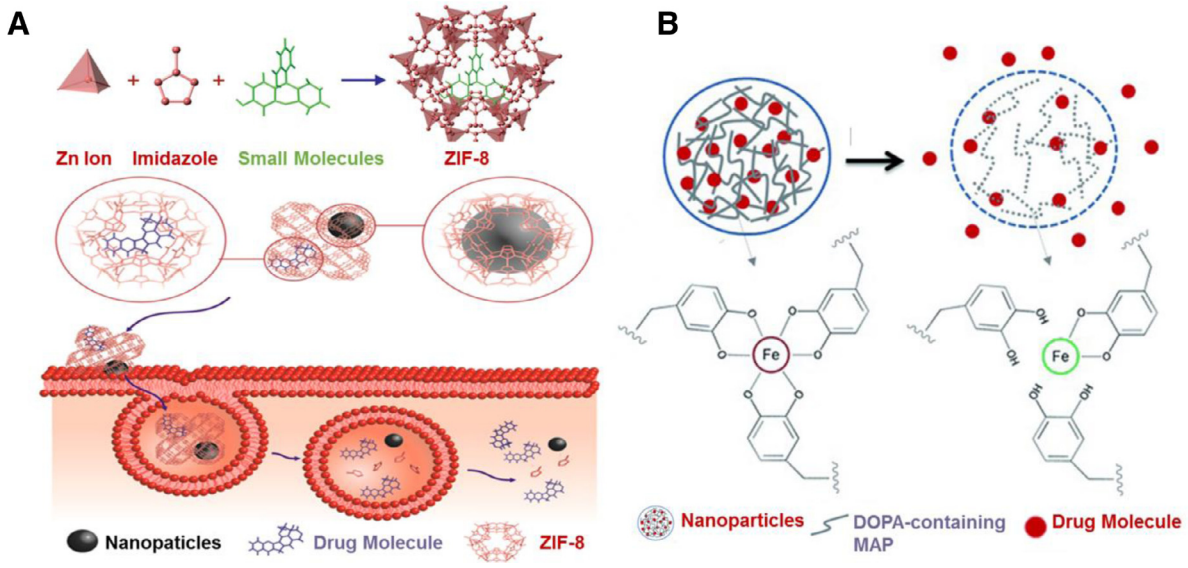

Fig. 4 – pH responsive DDSs. (A) Encapsulation of small molecules into the ZIF-8 frameworks during synthesis, and acidic responsive release of drugs or NPs at tumor microenvironments (Reproduced with permission from [58]. Copyright 2014, American Chemical Society). (B) Recombinant of DOPA-containing MAP and Fe (III)-DOPA complexation for pH-triggered drug release (Reproduced with permission from [61]. Copyright 2015 Wiley-VCH). (For interpretation of the references to color in this figure legend, the reader is referred to the web version of this article.)

in turn was depended on the wall composition of the capsules. Owing to the discoidal shape of these capsules, they showed dramatically decreased cellular internalization ratio compared with circular capsules, which might provide a solution for the decrease of nonspecific interaction during systemic circulation. But their size in micrometers remains to be challenging for further application as drug carriers. Cholesteryl hemisuccinate (CHEMS) with pKa around 5.8 is another material widely applied in the construction of pH sensitive liposomes [64]. It is the esterification products of cholesterol β-alcohol and succinic acid [64]. The acid-responsive property of CHEMS attributes to the protonation of carboxyl groups, which changes the spatial structure of liposomes composites and promotes drug release from the liposomes [64]. Poly [2-(diisopropylamino) ethyl methacrylate] (PDPA) and its derivates with a wide pKa range between 4.0 and 7.4 is also an important pH-responsive protonated polymer [65]. Examples include amphiphilic PEG-b-PDPA copolymer [66] and poly [2-(diisopropylamino) ethyl methacrylate]-b-poly [(ethylene glycol) methyl ether methacrylate] (PDPA-b-POEGMA) [67]. These two copolymers had a pH transition at 6.2 and exhibited much sharper and quicker pH response in the acidic endocytic organelles than many previous pH-sensitive nanosystems [68,69]. Gao et al. reported star-like NPs where PDPA-b-POEGMA anchored on a β-CD core for simultaneous controllable drug delivery [67]. Due to the presence of the PDPA blocks, the copolymers were hydrophobic at pH 7.4 which enabled the efficient loading of hydrophobic drugs such as doxorubicin (DOX) in their hydrophobic layer, while an acidic environment (*e.g.* pH 5.0) could trigger the hydrophobicity-hydrophilicity transition of PDPA blocks to induce drug release for cancer therapy [66,67]. In another study by the same group, various analogues of PDPA containing tertiary amines with linear or cyclic side chains were utilized to delivery ovalbumin for cancer immunotherapy [70]. It turned out that PC7A NPs having a pKa around 7.9 and the highest OVA-specific cytotoxic through T lymphocyte response for splenocyte killing (82%). Based on the *in vivo* studies of C57BL/6 mice bearing B16F10 melanoma, MC38 colon and TC-1 cancer cells, the NPs exhibited an enhanced accumulation in lymph node and showed decreased tumor size together with increased survival days [70]. In another study, cationic poly (allyl amine hydrochloride) (PAH) with a pK_a of 8.3 was utilized to cross-link gold nanoclusters forming Au-GSH-PAH aggregates for pH dependent fluorescence imaging and drug delivery [71]. The electrostatic interaction between the amino groups of PAH and the carboxyl groups of GSH medicated the aggregation-induced emission process (AIE) of the aggregates. When pH lower than pK_a (8.3), fluorescence intensity was reduced because of the weak crosslinking interaction which was contributed to the aggregates' swelling. Decreasing the pH to 6.5 enabled the recovery of the initial fluorescence intensity which indicated the reversibility of particle swelling. Besides, successful intracellular delivery of molecules including antibodies and peptides was achieved in this platform, making the system a theranostic platform with great potential.

Meanwhile, endogenous biomolecules were also demonstrated as new carriers with pH responsiveness, including proteins [50,72,73] and DNA [74]. Ferritin is one of the popular acidic responsive proteins whose self-assemble promotes the formation of a hollow cage structure where metal ions especially Fe (II) can be bound. For effective entrapping of high molecular metal complexes, the channels of natural ferritin proteins are usually widened by e-helix

removal. Thus, the metal complexes can be loaded via simple incubation without destruction of the tertiary structure and function of the proteins. In a recent study, Jung's group developed ferritin nanocages with partially opened hydrophobic channels for loading of Fe (II)-DOX complexes [50]. It's demonstrated that the obtained ferritin protein was stable at pH 6.0 and started to disassemble at pH 4.0–5.0, imitating the endosomal pH of cancer cells. The acidic responsive disassembly of ferritin protein caused the metal complexes dissociating from the cavity and achieved on-demand cellular drug release. The pH (low) insertion peptide (pHLIP) is another popular acidic responsive peptide, whose insertion and span of tumor cell membrane are triggered by acidic microenvironment [72]. Cheng et al. developed a novel pHLIP-based platform where therapeutic nuclear acid analogues were attached via GSH-responsive disulfide bridge [73]. The pHLIP underwent protonation and increase in hydrophobicity of the peptide with exposure to acidic environments (pH $\approx$ 6). This accompanied with the spontaneous formation of helix structures which facilitated the insertion of the nanomedicine to cross the tumor cell membrane via a non-endocytic pathway. And followed by a GSH triggered cleavage of disulfide bond, the intracellular release of the nuclear acid analogues was achieved. *In vivo* studies of mouse lymphoma model demonstrated that the DDS could efficiently silent miR-155, showing a significant reduction in tumor growth and metastatic spread to other organs. Qiao et al. reported poly(L-histidine) based pH-sensitive micelles which exhibited excellent endolysosomal escape property [75]. When the micelles entered into lysosomes, the amine group of poly(L-histidine) became protonated and activated the function of proton pump [75]. This lead to the influx of water molecules and Cl^- ions, a rise of lysosomal osmotic pressure and swelling up of the lysosomes, resulting in the release of the encapsulated drug into cytoplasm [75]. In another study, oligodeoxynucleotides (ODNs) attached gold nanoparticles were applied for acidic responsive co-delivery of DOX and antisense ODNs to bcl-2 mRNA [74]. In detail, the antisense ODNs and i-motif binding ODNs were first anchored onto the surface of the AuNPs, and another cytosine-rich i-motif sequence served as the linker for the co-assembly of these gold nanoparticles. The resulted DNA duplexes rich in guanine and cytosine base pairs provided accommodation for DOX. At acidic environment (pH = 5.0), the i-motif sequence formed a unique tetrameric structure by partial hybridization of cytosine and protonated cytosine, resulting in disassembly of the gold clusters, which accompanied with the release of DOX and enhanced exposure of antisense ODNs. *In vivo* studies of A549-bearing nude mice xenograft demonstrated that the AuNPs clusters showed 2.5-fold higher tumor accumulation and lower accumulation in other organs than single AuNPs and exhibited efficient inhibition of tumor growth. In addition, some inorganic materials, for example, calcium carbonate ($CaCO_3$) [52], zinc oxide (ZnO) [54,76], and manganese dioxide (MnO_2) [77], are relatively insoluble at neutral environments, but can be dissolved as nontoxic ions under acidic condition, making them potential acidic sensitive materials. Zhong et al. developed a ZnO-functionalized theranostic nanoplatform for clear tri-modality bioimaging and acidic responsive on-demand DOX release [76]. Here, lanthanide-doped upconverting NPs (UCNPs) were endowed with rich optical and magnetic properties as well as strong X-ray attenuation, allowing UCL/CT/MRI tri-modality imaging. For introduction of acidic responsiveness, the UCNPs were coated with mesoporous silica layer where ZnO served as the "gatekeepers" (gatekeepers are plugged within the pores of silica to control drug release). The platform showed an extremely slow DOX release behavior at pH 7.4 whereas a remarkable drug release was observed at pH 5.0. Besides, *in vitro* and *in vivo* imaging studies demonstrated the successful construction of the tri-modality system. These complementary results proved that the platform was a promising candidate for cancer theranostic.

3.1.3. *Gas generating based systems*

Gas generation is another novel strategy for acidic responsive DDS design. HCO_3^- is the most studied substance capable of reacting with acid for carbon dioxide gas generation. Thus, materials with HCO_3^- possess great potential for acidic sensitive drug delivery. Early in 2012, Liu et al. reported a new liposome system which can delivery anticancer drug into tumors with an acidic responsive drug release profile [78]. In the platform, DOX together with bicarbonate ion was encapsulated into the liposomes. At acidic environment (pH 5.0), which mimics the acidic environment in lysosomes, the generation of carbon dioxide gas was triggered causing effective drug release from the liposomes. This gas generation strategy was also applied for the reversion of P-glycoprotein-mediated multidrug resistance (MDR) by Chung et al. [79]. They developed an injectable PLGA hollow microsphere (HM) loaded with anticancer agent irinotecan (CPT-11, a camptothecin derivative) and a NO releasing donor (NONOate). The key composite of this system was NO releasing donor which can react with environmental proton at pH 6.6 to generate NO bubble. The NO bubble acted as P-gp-mediated MDR reversal agents based on the reduction of P-gp expression level. Meanwhile, when the pressure of NO reached a certain level, the HMs shell was disrupted and pores were formed, allowing the burst release of the encapsulated CPT-11. The group investigated the *in vivo* drug release behavior of Cy5-loaded HMs which exhibited a much stronger fluorescence intensity in MCF-7/ADR tumor than that of the normal tissue. In addition, the tumor model mice injected with the HMs significantly suppressed tumor volume while free CPT-11 group exhibited minimal antitumor activity against the MDR tumors. Thus, both efficient MDR reversal and drug release were achieved via the HMs.

3.2. *GSH-triggered drug delivery systems*

GSH is a tripeptide thiol composed of glutamate, cysteine, and glycine in the cytoplasm of living cells, of which the physiological redox process is based on GSH/GSSG system. The concentration of GSH in the cell (1–10 mM) is 100–1000 times higher than that in the extracellular space (1–10 μM) [80]. More importantly, compared with healthy cells, the level of GSH is about fourfold higher in cancer cells [81]. Perry et al. gave a comprehensive summary of the gluthione levels in different tumor types [82]. It's found that ovarian, head and neck, lung, brain and breast tumors have similar GSH levels in the range of 10–

Table 2 – Representative redox-responsive polymeric materials and their responsive mechanisms.

Functional Groups	Redox-responsive mechanisms
Sulfide [99,101,117]	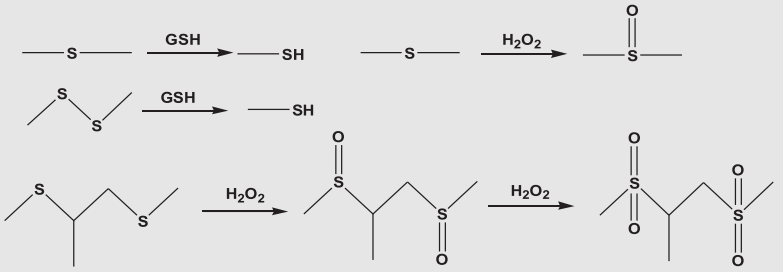
Selenium [96,97,119]	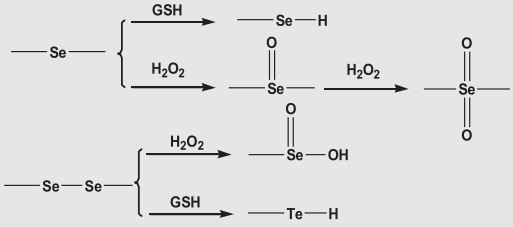
Telenium [95,118]	
Boronic ester/acid [122,123]	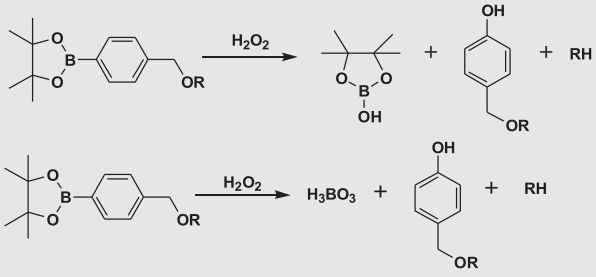
Thioketal [124,125]	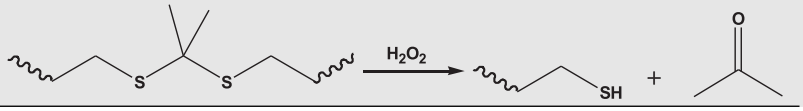

20 nmol/mg protein, while colorectal tumors exhibited a much higher GSH level around 90 nmol/mg protein [82]. This indicates that colorectal tumors have a higher responsiveness toward GSH triggered DDSs than other tumor types. These concentration contrasts are generally harnessed to tune the carrier's "stability" which endows the NPs with long circulation time and programmed intracellular molecules release. High intracellular GSH concentration should be adequate enough for degradation of certain chemical linkages [83]. In the last few years, numerous functional moieties have been successfully applied in construction of GSH-responsive carriers. Here we divide these groups into five types, namely disulfide, diselenide/ditelluride, thioether/ selenide/tellurium, metal-thiol based linkers and ferrocenium. Some GSH responsive groups and their related mechanisms are listed in Tables 2.

3.2.1. *Disulfide*

Disulfide can be readily incorporated into polymers through fairly straightforward chemistries, such as L-cystine [84], dithiodiglycolic acid [85], and pyridyl disulphide chemistry [86], thus contributing to the development of substantial carriers, such as nanogels [87], micelles [88], polymersomes [89] and mesoporous silica NPs [90]. In most cases, these carriers are fabricated with pendant disulfide bridges, which enable an intracellular GSH-triggered thiol-disulfide exchange. Wang et al. developed a sarcoma-targeting polypeptide-decorated disulfide-crosslinked nanogel (STP-NG) for intracellular delivery of shikonin to inhibit osteosarcoma progression [87]. In the presence of 10.0 mM GSH, almost 98.4% of the shikonin was released from the nanogel within 72 h due to the dissolution of disulfide bond (S–S) [87]. Further, *in vivo* studies revealed that the nanogel could selectively accumulate in orthotopic 143B osteosarcoma and exhibited great antitumor efficacy and inhibition of pulmonary metastasis via necroptosis [87]. Lin et al. reported GSH responsive polymeric micelles for reversion of cisplatin (cis) resistance attributed to upregulated intracellular GSH level [88]. The micelles contained poly (disulfide amide) with high disulfide density which enabled efficient scavenging

of the cytosol GSH for activation of the detoxification pathway, and consequently reduced the likelihood of released cisplatin drugs being deactivated (Fig. 5A). In A2780CIS tumor-bearing athymic nude mice model, the micelles displayed decreased tumor growth, with tumor inhibition rates as 83.32% ± 5.80% *versus* 1.48% ± 0.53% for the control NPs, and 1.46% ± 1.29% for free cisplatin, respectively. Furthermore, the hydrophobicity of the polymers can be well-tuned by aromatic group introduction or alkyl chain length change, leading to optimization of micelles properties including particle size, Pt loading capacity and drug release behavior.

In another study, GSH responsive stomatocyte nanomotors of poly (ethylene glycol)-SS-polystyrene (PEG-SS-PS) polymersomes were developed for the delivery of DOX (Fig. 5B) [89]. Nanomotors are nanoscale devices capable of converting energy into movement, consequently endowing the DDS with propulsion feature along certain gradients of chemical signaling molecules. In this system, Pt NPs catalysts were encapsulated into the cavity whereas DOX was loaded into the lumen of the stomatocyte. Propelled by the H_2O_2 gradients in the body, the nanomotors were able to migrate toward the diseased area. Subsequently the concentrated GSH infiltrated into the lumen of the nanomotors to cleave the disulfide bonds and resulted in the cleavage of the PEG shell. This was accompanied with motility loss of the nanomotor and in-site drug release. However, these stomatocyte-mimicking platforms possessed a size around 349 nm, still limiting their practical application as DDS. In addition, Du et al. developed poly (γ-glutamic acid) (γ-PGA)-coated mesoporous silica nanoparticles (MSNPs) for GSH responsive DOX delivery. In detail, MSNPs were attached with amine functional DOX via disulfide bonds, and then γ-PGA coating was achieved based on sequential electrostatic adsorption of nontoxic poly(ethylenimine) (PEI). A decrease in pH from 7.4 to 5.0 promoted the protonation of γ-PGA, which resulted in the electrostatic repulsion between γ-PGA and cationic PEI layer. Also, intracellular GSH dissociated the DOX from the mesoporous NPS. And via the loose polyelectrolyte coatings, the detached DOX diffused into the cytoplasm for therapeutic effects.

Sun et al. developed three novel paclitaxel (PTX)-citronellol (CIT) prodrugs conjugated via diverse lengths of disulfide-containing carbon chains and conducted an in-depth investigation on how the position of disulfide bonds affects the redox responsiveness [91]. The disulfide bonds locate at α-, β- or γ-positions, respectively, in the carbon chain, denoted as α-PTX-SS-CIT, β-PTX-SS-CIT, and γ-PTX-SS-CIT (Fig. 6A–6C) [91]. It was demonstrated that the β-PTX-SS-CIT showed a slower drug release than α-PTX-SS-CIT and γ-PTX-SS-CIT, while the oxidation-responsiveness of the prepared prodrug followed the order of γ-PTX-SS-CIT < β-PTX-SS-CIT < α-PTX-SS-CIT [91]. In another study, the group further studied the synergistic influence of carbonate and carbamate linkage on the disulfide bond-driven redox responsiveness (Fig. 6D) [92]. The hydrolysis of the carbonate linkers was confirmed to be easier than carbamate linkers [92].Thus, based on the rational selection of the conjugation types, the release profile of the prodrugs can be finely tuned.

3.2.2. *Ditelluride/diselenide bond*

The energy of Te–Te bond and Se–Se bond is estimated to be 149 and 192 kJ/mol, respectively, which is lower than that of the S–S bond (240 kJ/mol), suggesting that the diselenide/ditelluride-containing polymers can be more easily cleaved by either oxidation to form selenic/telluric acid or reduction to form selenol/tellurol in different redox environment [93,94]. Among the three covalent bonds mentioned above, Te–Te bond with the lowest energy holds excellent potential in the construction of ultrasensitive drug carriers. Wang and coworkers first reported ditelluride-containing poly (ether-urethane) NPs for GSH responsive drug delivery [95]. DOX was used as the model drug and might be attached to the hydrophobic segments of the NPs via hydrophobic interactions. In this case, sensitive ditelluride could be rapidly reduced to tellurol in the presence of GSH (10 mM) within 5 min, leading to dissociation of the NPs, while the group without GSH treatment didn't show obvious aggregation. *In vivo* biodistribution studies in 4T1 tumor mice model demonstrated that a larger amount of the Te-DOX NPs accumulated at tumor site compared with the free DOX and C6-DOX. The tumor volume of the model was estimated to be 3 folds for Te-DOX NPs, 6.7 folds for C6-DOX, 6.2 folds for free DOX and 13 folds for free DOX until the 19th day, indicating the NPs with a much stronger inhibition of tumor growth than the control groups. A similar GSH-responsive polymer with diselenide group was developed by Xu et al. A triblock polymer was assembled into micelles in water and exhibited unique dissociation upon redox treatment [96]. In a recent study by Shao's group, a diselenide-bond-containing organosilica precursor was applied in the synthesis of large pore-sized MSNPs for the delivery of bio-macromolecules [97]. The obtained MSNPs had Si-C, Si-O and Se-Se bonds on their surface. Among them, Si-C bond is much weaker and was selectively broken up by hydrothermal treatment to form a large pore size (~11.3 nm) which is suitable for protein encapsulation. For homologous targeting, cancer cell membrane was coated on the protein-loaded MSNPs. Compared with controlled disulfide MSNPs, the selenium group exhibited a similar release trend after GSH treatment (5 mM), but a higher one after H_2O_2 treatment (100 μM). The group further examined the therapeutic efficacy of the NSNPs on the female nude mice bearing orthotopic HeLa tumors. It's demonstrated that the MSNPs with cell-membrane cloaking showed significantly reduced tumor volumes and tumor weights compared with the NPs without cell-membrane cloaking or the free RNase A group. And thus, it might provide a new insight for the development of carriers to overcome tumor redox heterogeneity.

3.2.3. *Thioether/selenide/tellurium*

Thioether-containing polymers were generally obtained via Michael-type addition of thiols with maleimide. In response to elevated GSH, the resulted polymers undergo retro-Michael reaction and thiol exchange, further leading to accelerated carrier degradation and drug release. Early in 2013, Kiick and colleagues reported a PEG-heparin hydrogel, in which maleimide-functionalized heparin was crosslinked with various thiol-functionalized PEG polymers through succinimide-thioether linkages [98]. Oscillatory rheology experiments confirmed the stability of the resulted hydrogels. Compared with disulfide-crosslinked hydrogels, the succinimide-thioether hydrogel exhibited 10-fold slower rates of degradation, indicating these Michael-type addition

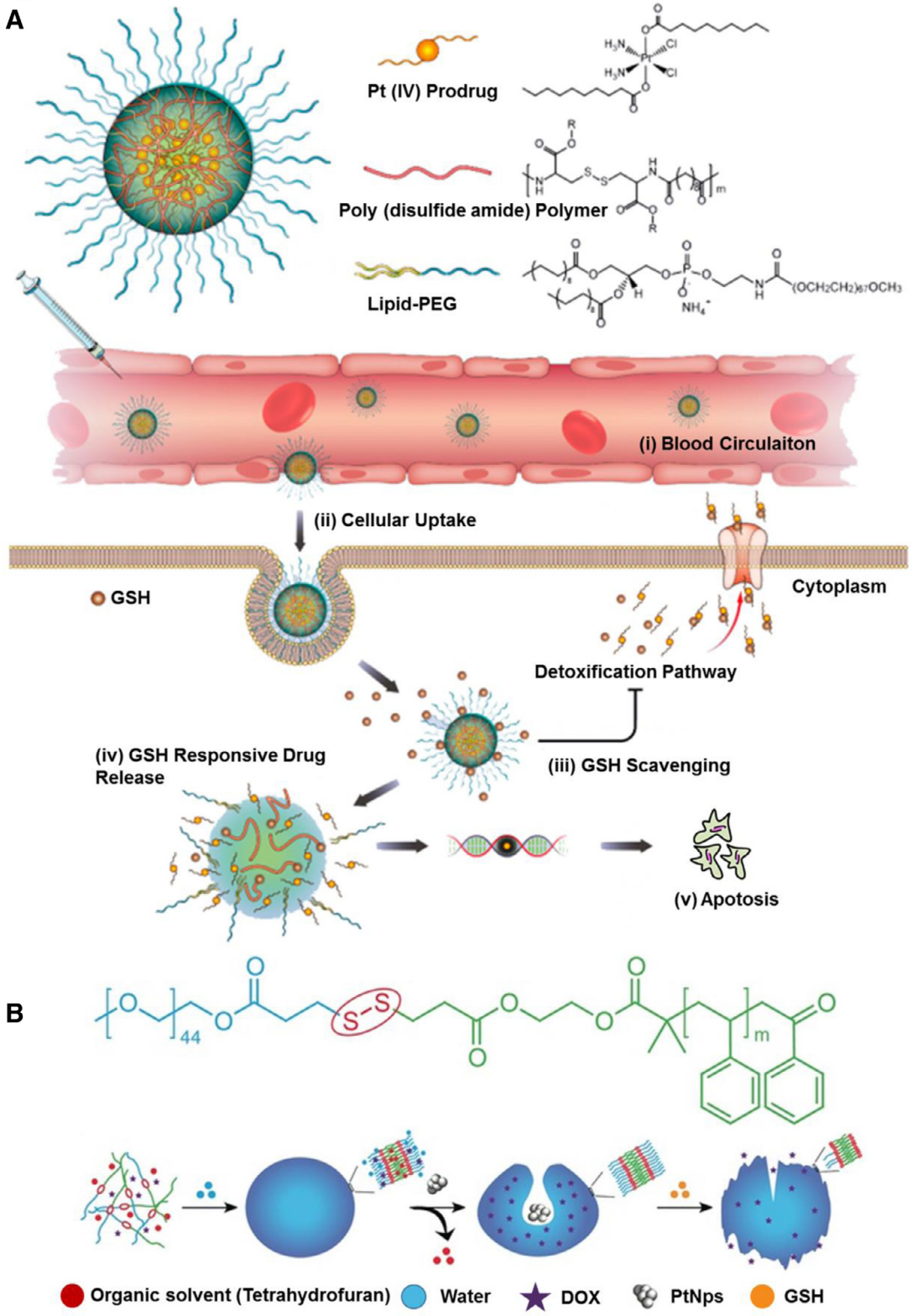

Fig. 5 – GSH responsive DDSs. (A) Illustration of the gluthione-triggered nanoplatform, comprising Pt (IV) prodrug, poly (disulfide amide) polymers and lipid-PEG for treatment of cisplatin-resistant tumors; Intracellular delivery of Pt and reversal of tumor cisplatin resistance (Reproduced with permission from [88]. Copyright 2018, American Chemical Society). (B) Chemical structure of the redox-responsive block copolymer PEG-SS-PS used for the stomatocyte assembly; Self-assembly and GSH-triggered disassembly of the redox-sensitive stomatocyte nanomotor (Reproduced with permission from [89]. Copyright 2017 The Authors). (For interpretation of the references to color in this figure legend, the reader is referred to the web version of this article.)

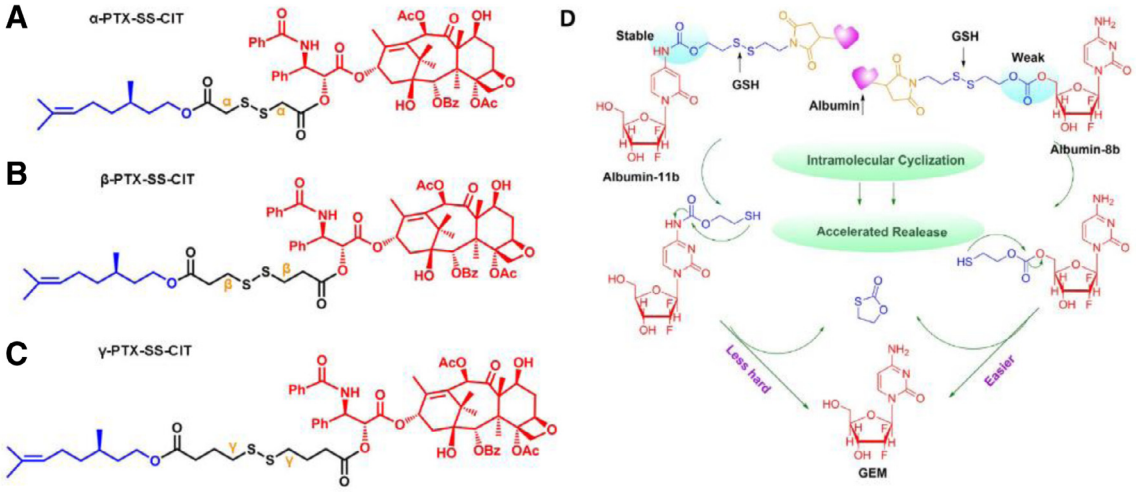

Fig. 6 – Chemical structures of the disulfide-containing PTX-CIT prodrugs: (A) α-PTX-SS-CIT, (B) β-PTX-SS-CIT, and (C) γ-PTX-SS-CIT (Reproduced with permission from [91]. Copyright 2018 American Chemical Society). (D) Drug release of carbonate- and carbamate-linkers bearing albumin-prodrug conjugates after intravenous administration (Reproduced with permission from [92]. Copyright 2018 American Chemical Society).

products had enhanced blood stability and prolonged circulation time. Later, the group fabricated a liposome-crosslinked hybrid hydrogel with GSH responsiveness based on Michael-type addition [99]. In this case, they integrated maleimide-functionalized liposome nanoparticle and aryl thiol-functionalized 4-arm PEG polymer into a unifying hydrogel network through thioether succinimide cross-linkers. The multiple domains within the gel allowed dual loading of DOX and cytochrome c (cyto-c) which can be loaded in the liposomes and the bulk polymer network, separately. In response to 10 mM GSH, the gel exhibited simultaneous release of DOX and cyto-c with differential trend. Such hybrid systems conserved the structural integrity and functionalities of the incorporated NPs, offering exclusive benefits including diminished burst release and controlled sequential delivery.

The thioether groups exhibit both GSH and H_2O_2 responsiveness. Wang et al. introduced thioether into docetaxel prodrugs to resist breast cancers [100]. Compared with single stimuli sensitive DDSs, the system showed a faster release of docetaxel because responding to two opposite stimuli [100]. Compared with free DTX, the redox dual-responsive platform had comparable cytotoxic activity [100]. Besides, the antitumor efficacy was estimated in 4T1 tumors bearing mice. It turned out this nano assemblies could enhance anticancer efficacy by increasing the dose because of higher tolerance [100]. In another study by Luo et al., an in-depth exploration of the correlation between linker variations (thioether, dithioether and ester bond) of materials and *in-vivo* redox responsive release profile of paclitaxel (PTX) was conducted [101]. They conjugated PTX to oleic acid (OA) with long unsaturated alkyl chains via three linkers mentioned above, denoted as PTX-S-OA, PTX-2S-OA and PTX-OA, separately. These three polymers were self-assembled into NPs, onto which tocopheryl polyethylene glycol 2000 succinate ($TPGS_{2k}$) was coated for prolonged circulation time (Fig. 7A). The PTX-S-OA exhibited superior redox sensitivity over PTX-2S-OA, achieving more rapid and selective release of free PTX from the prodrug NPs triggered by redox stimuli. It indicated that the sulfur atom close to the ester bond with drug attached was the key component for controlling of the redox-sensitivity in the dithioether polymer, rather than the one remote from the ester bond (Fig. 7C and 7D). Fig. 7B gives a detailed description of redox responsive mechanisms of PTX-S-OA. Cellular GSH initialized the thiolysis process, facilitating PTX release from the prodrug, and ROS triggered the oxidation of the thioether groups to hydrophilic sulfone, making the proximal ester bond more easily hydrolyzed. And the decreased steric hindrance of the oleic acid 2-hydroxyethyl ester further promoted its first removal of long lipophilic OA chain, followed by the hydrolysis of the ester bond linked with PTX for ROS responsive drug release. In addition, the PEGylated PTX-S-OA NPs with considerately high drug loading around 57.4% showed potent antitumor activity in a human epidermoid carcinoma xenograft.

Mono selenide and telluride are also interesting functional moieties with GSH responsiveness. In 2012, Xu's group reported a selenide-containing amphiphilic polyurethane (PU) which could be self-assembled into micelles for GSH responsive Pt delivery [102]. In particular, the coordination chemistry between Pt and selenide atom allowed the attachment of Pt-based drugs. Through the competitive coordination of GSH (10 mM) to Pt^{2+}, the micelles exhibited interesting disassociation profile concomitant with cargo release. Later, the group reported a similar micelle self-assembled from tri-block polymer with mono telluride groups for GSH triggered Pt delivery [103]. The key compartment of this system was the coordination interaction between Pt and telluride which not only allowed the accommodation of Pt but also underwent detachment of the drugs in the presence of GSH (10 mM). In a recent study, He et al. synthesized six paclitaxel-citronellol conjugates using either thioether bond, disulfide bond, selenoether bond, diselenide bond, carbon

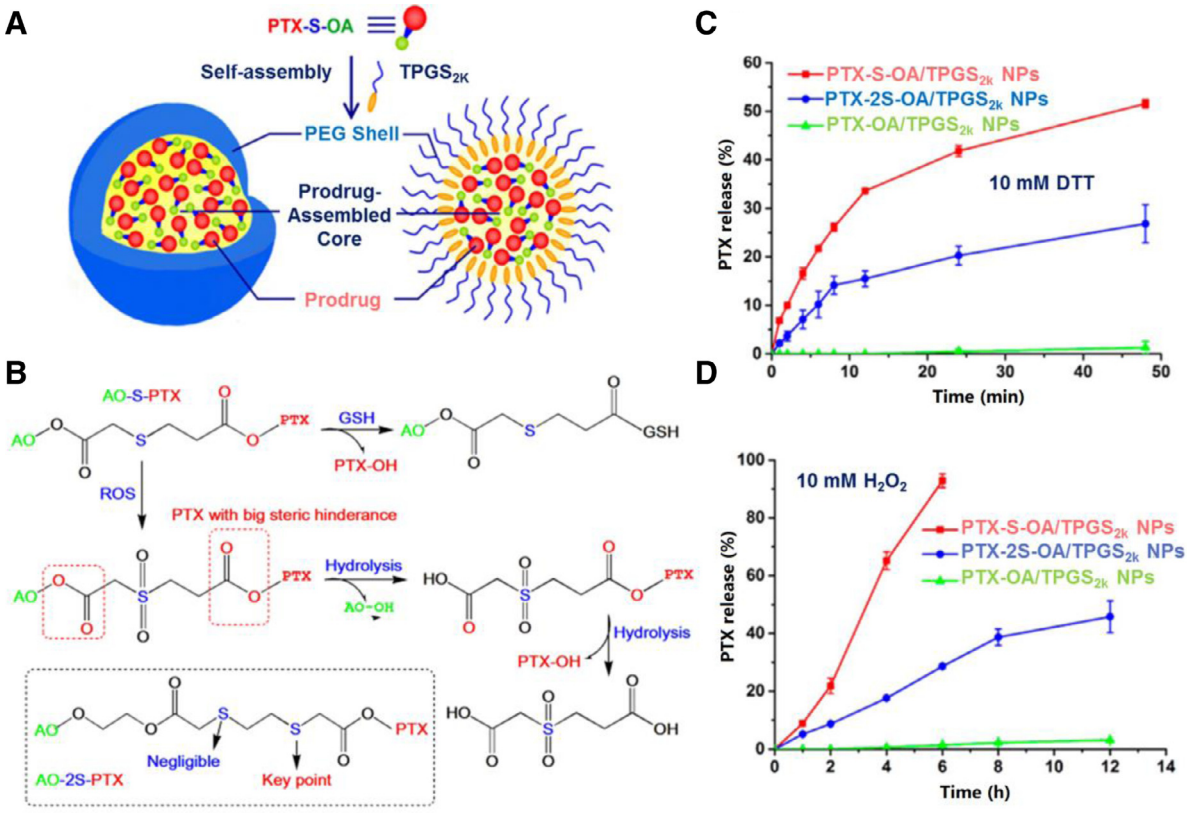

Fig. 7 – GSH responsive DDSs. (A) Preparation of PEGylated prodrug NPs of PTX-S-OA; (B) Redox-sensitive drug release of PTX-S-OA triggered by GSH/ROS; PTX release from PTX-S-OA/TPGS$_{2k}$ NPs, PTX-2S-OA/TPGS2k NPs and PTX-OA/TPGS2k NPs after treatment with (C) 10 mM DTT and (D) 10 mM H_2O_2 (Reproduced with permission from [101]. Copyright 2018 American Chemical Society). (For interpretation of the references to color in this figure legend, the reader is referred to the web version of this article.)

bond or carbon-carbon bond as linkages [104]. Specially, the influence of these linkers on prodrugs efficiency was investigated. It turned out that bond angles/dihedral angles had remarkable influence on the redox-responsivity of these sulfur/selenium/carbon bonds, which could further affect the stability and pharmacokinetics of the prodrugs. What's more, selenoether/diselenide bond could produce ROS to improve the cytotoxicity of these prodrugs.

3.2.4. *Metal-thiol based bond*

Thiol-containing biomolecules exhibit strong affinity with noble metal NPs including Au and Ag. These biomolecules could not only stably protect them but also control the self-assembly process of these special NPs via metal-thiol based linkage. Wang et al. synthesized dendrimer-coated gold NPs (DEGNPs) which were used as carriers for thiolated anti-cancer drugs [105]. Since there are plenty of "pockets" remaining in DEGNPs, these NPs could be loaded with sulfhydryl-containing drugs via electrostatic, hydrophobic and/or van der Waals interactions. Besides, other functional groups on anticancer drugs such as amine, hydroxyl, and carboxyl can be easily converted to the thiol group, and further attached to the surface of the gold NPs through Au-S bond. The resulted Au-S bond contained in DEGNPs exhibited a detached release behavior in the presence of thiol reducing agents such as glutathione and dithiothreitol to achieve controlled release. GSH-responsive DEGNPs increased the therapeutic efficiency of the loaded drug. Ag-S bond was also utilized for the selective and sensitive detection of thiol-containing biomolecules like GSH [106]. In this case, silver NPs were loaded onto carbonaceous nanospheres. And based on Ag-S bond, fluorescein isothiocyanates with S=C=N- groups were further attached onto the hybrid spheres. Thiol containing biomolecules can competitively bind to the AgNPs, and resulted in the release of the fluorescein isothiocyanate. According to their fluorescence intensity, the concentration of the thiol containing molecules can be detected. It's confirmed that the linear detection range for GSH was 0.02–1 μM, where the abnormal GSH concentrations in cancer cells were covered.

3.2.5. *Ferrocenium*

Ferrocenium/ferrocene redox couple provides another alternative strategy for the development of GSH responsive DDS. Their GSH sensitive mechanisms are based on the polarity shift resulted from the reduction from ferrocenium cation to ferrocene, where the shift is the driving factor for vesicles' assembly and disassembly. According to this unique feature of ferrocene, Wu et al. developed a redox-responsive system for co-delivery of anticancer drug and siRNA [107]. Specially, amphiphilic pillararenes (APs) served as carriers and provided numerous cavities for cargo

encapsulation. And then they conjugated ferrocenium cation head groups to APs, enabling the carrier with positive charged surface. The amphiphilic hybrid polymer was assembled into monolayer vesicle. Thus, this platform was endowed with co-delivery ability where vesicle cavities for anticancer cargo loading and positive charged surface for negatively charged siRNA binding. In addition, vesicles are GSH responsive dissociation. In a recent study, Liu's group reported another GSH responsive micelles self-assembled from amphiphilic ferrocenium-hexane-nitroimidazole (Fe-NI), onto which, HA shell was coated based on electrostatic interactions [108]. Nitroimidazole (hypoxic cell radiosensitization) and DOX (inhibition of tumor growth) were co-loaded within the micelles for the treatment of radiotherapy (RT) resistant hypoxic tumor. In the presence of GSH (10 mM), the hydrophilic ferrocenium cation reduced to hydrophobic ferrocene, resulting in the disassembly of micelles and followed by the release of the encapsulated cargoes. The group further studied the *in vivo* antiglioma efficacy in mice bearing PC3 tumors. It turned out that the mice group treated with DOX and nitroimidazole showed remarkably enhanced cell apoptosis and lowest tumor weight compared with the control groups.

3.3. *ROS-triggered drug delivery systems*

ROS, including H_2O_2, O^2•, •OH, $ONOO^-$, OCl^- and etc., play crucial roles in a number of cell metabolic pathways [109]. However, the imbalance of ROS leads to oxidative stress and inflammatory events, which are often associated with pathological effects such as cancer [110], inflammation [111,112], diabetes [113], neurodegeneration [114]. As the main component of the intracellular oxidate, typical H_2O_2 level in normal tissue is tightly regulated around 20 nM, while in cancer tissues, it's as high as 50–100 μM due to excess H_2O_2 accumulation [115]. Despite the fact that this concentration contrast between normal and cancer cells is much sharper than GSH, very few of ROS responsive moieties exhibited sufficient sensitivity at tumor cellular concentrations (50–100 μM) for controlled drug release. This could be attributed to the fact that the ROS in tumor cells are not effective in inducing the break of chemical bonds. For example, mono-sulfide and polysulfides had a responsive concentration greater than 1 mM [116,117] and even ultra-sensitive mono-tellurium and diselenide only exhibited a responsive concentration of 100 μM [118,119]. Thus, ROS produced by NPs were generally cooperated with the endogenous ROS to control carrier "stability" for site-specific drug release. In this section, the reported materials are classified into two types, namely amphiphilicity transition model and bond cleavage model based on the responsive mechanisms. Also, two strategies are introduced for amplification of ROS concentration in tumor, namely photodynamic therapy (PDT) and ROS producing agent treatment. Some typical H_2O_2 responsive groups and bonds are listed in Table 2.

3.3.1. *Amphiphilicity transition*

Amphiphilicity is one of the molecular basics for NPs self-assembly. Polymers with hydrophobic mono-sulfide [116], mono-selenium [96], or mono-tellurium groups [96], are capable of forming hydrophilic oxidative products in response to H_2O_2. This hydrophobic-to-hydrophilic transition will destroy the balanced amphiphilicity of the NPs, accordingly leading to structural dissociation and subsequent cargo release. Xu's group developed a series of PEG-PU_X-PEG triblock polymers for redox responsive cargo delivery, wherein X could be S atom, Se atom, Te atom, or Se-Se bond [96]. And the Se atom, Te atom, and Se-Se bond with GSH responsiveness have been introduced in the previous chapter. The C-S and C-Se bond, whose energy was estimated to be 272 and 244 kJ/mol, respectively, were applied in oxidate triggered drug delivery by the group. It's demonstrated that in the presence of H_2O_2 (0.1%, v/v), most of the selenide groups could be converted to selenones (O=Se=O), but only a very small portion of sulfide groups were able to be transformed to low oxidation state (S=O) at the same condition within 5 h oxidation. The results indicated that the C–Se bond was more sensitive to H_2O_2. Yang et al. constructed a ROS-responsive prodrug nanoplatform where 6-maleimidocaproic acid (MAL) was conjugated to PTX via mono-sulfide linker, leading to the self-assembling of the PTX-S-MAL prodrug into uniform size NPs [116]. It was demonstrated that the conjugated drugs were efficiently released from the NPs with the concentration of H_2O_2 greater than 1 mM [116]. In another study by Duvall's group, sulfide-containing poly (propylene sulfide) (PPS) NPs were leveraged for curcumin delivery [117]. H_2O_2 with a concentration level within 0.5–500 mM successfully triggered a morphological transition of the hydrophobic PPS-based NPs to more hydrophilic poly (propylene sulfoxide) and poly (propylene sulfone), making it a good candidate for on-demand drug delivery. However, all of the three platforms exhibited insufficient sensitivity to control the efficient drug release at tumor cellular concentrations of ROS (50–100 μM), which is too low to trigger reactions *in vivo*, thus limiting their clinical applications.

In 2015, an ultra-sensitive ROS-responsive material was developed by Wang et al. [118]. This material exhibited H_2O_2 responsive profile at the concentration of 100 μM. The group integrated the ultra-responsiveness of tellurium-containing molecules and biocompatibility of phospholipids (DPPC) into a unifying nanostructure. The diameter of the nanostructure exhibited a correlated increase with the increase of tellurium moieties content. ^{1}HNMR and ESI-MS negative spectrum demonstrated their hydrophobic-to-hydrophilic transition and the formation of one oxygen atom added structure upon H_2O_2 addition. More interestingly, the transition was recovered after mild reductants addition such as vitamin C. It indicated that the oxidation and reduction process could be repeated with certain circles. Later, Park and coworkers reported another ultra-sensitive polymeric micelles composed of diselenide-crosslinkers, which responded to H_2O_2 at a concentration of 100 μM [119]. Different from the two bonds mentioned above, the responsive mechanism of this platform was based on ROS sensitive cleavage of Se–Se crosslinks, which generated hydrophilic selenic acid. This accompanied with dissociation of the micelles and subsequent drug release. In PC3 tumor-bearing mice, the micelles delivered 3.73-fold and 1.69-fold higher drug amount compared with free drug and their non-crosslinked counterparts, respectively, and effectively inhibited tumor growth.

PDT is a common strategy for generation of cytotoxic ROS. It consists of two procedures: accumulation of photosensitizers within the target site and their photoactivation to produce ROS. The combination of PDT (just for generation ROS) and ROS responsive carriers provides a solution for insufficient biological concentration of ROS. Dong et al. reported degradable NPs (denoted as Pros-PDC NPs) loaded with DOX and IR780 (photosensitizers) (Pros-PDC) (Fig. 8A) [120]. The NPs contained two functional copolymers: one with ROS sensitive thioether chains and the other with acid-labile β-carboxylic amide pendants. When pH changed from 7.4 to 6.0, the NPs underwent a surface charge transition from negative to positive for enhanced internalization. Under laser irradiation, IR780 was able to efficiently produce ROS and trigger the oxidation of the thioether chains, therefore, resulting in the disassembly of NPs and subsequent DOX release. It's worth noting that the drug release profile was dependent on when and how long the laser irradiatreverseion was performed. Based on these, precise control of spatiotemporal drug release could be achieved. In 4T1 tumor-bearing mice, the Pros-PDC with laser showed a remarkable decrease of tumor size, indicating that ROS activated DOX release of Pros-PDC NP by light for reinforcement on the anticancer efficacy. Using a similar strategy, Sun's group designed a ROS-responsive prodrug nanoplatform co-encapsulated with pyropheophorbide as photosensitizers [121]. In this case, cabazitaxel (CTX) served as the model drug and conjugated with oleic acid (OA) via thioether-/selenoether linkers [121]. With the collaboration of both endogenous tumor-overproduced ROS and exogenous pyropheophorbide-generated ROS, these two linkers were efficiently cleaved and resulted in effective drug release [121]. Furthermore, the selenoether linkage was demonstrated with significant advantages over the thioether linkage in drug release rate and cellular cytotoxicity [121]. In 4T1 murine breast subcutaneous tumor models, the prepared prodrug significantly prolonged the circulation time and tumor distribution of both CTX and pyropheophorbide, thereby demonstrating excellent synergistic chemo-photodynamic therapy *in vivo*.

3.3.2. *Bond cleavage*

Bond cleavage is another common mechanism for NPs dissociation. In this case, the functional bonds are completely cleaved in response to H_2O_2, and upon structure disruption, the encapsulated drugs can be released. Typical examples of this responsive model include boronic acid and poly (thioketal).

Aryl boronic acid bond is an important building block for construction of ROS responsive carriers [122,123]. Upon H_2O_2 oxidation, these functional moieties can be cleaved, generating phenol and boronic acid as byproducts. In a study by Wang et al., aryl boronic acid was applied for reversible anticancer protein restoration [123]. RNase A served as the model protein whose activity is dependent on its lysine residues. In their work, amino group of the lysine residue was modified with aryl boronic ester (NBC) via carbamate ester linker thus leading to the decrease of protein activity to 5%. After H_2O_2 treatment, the conjugated acryl boronic ester underwent a self-driven reaction, releasing lysine and restoring protein function to 95%. In addition, RNase A lysine conjugation with NBC reversed the surface charge of RNase A from positive to negative, where cationic lipid NPs were able to be co-assembled via electrostatic binding. The cationic lipids served as shielding for acryl boronic ester during circulation. They were also able to target the cell membrane through electrostatic interaction thereby facilitating cell internalization. Despite the merits mentioned above, the NPs with positive charged surface were prone to be eliminated by the RES systems. Thus, more efforts should be taken to ensure further optimization of this platform.

Thioketal bond can also be cleaved by H_2O_2, leading to the scission of the polymer chain with acetone as an oxidation product [124,125]. Farokhzad et al. reported an innovative poly (thioketal)-based poly-prodrug for ROS-triggered mitoxantrone (MTO) delivery [125]. This platform contained three vital components: polyprodrug inner core with thioketal groups for ROS responsive drug release; PEG outer shell for prolonging circulation time; and surface-attached internalizing RGD (iRGD) for tumor targeting. These individual components could coassemble into spherical NPs with a diameter of 92 nm. The H_2O_2 cleavage process broke the thioketal groups, and released intact anticancer drug, which showed significant inhibition of cancer cell growth. The polyprodrug NPs coated with iRGD ligand were efficiently internalized by cancer cells.

As mentioned previously, very few of the reported moieties exhibited sufficient sensitiveness to trigger reaction at biological ROS concentration. In addition to PDT, ROS-producing agents without photo activation provide another approach for amplification of the intracellular ROS level. These ROS-producing agents such as copper ions [126], α-tocopheryl succinate (α-TOS) [127] and palmitoyl ascorbate [128] are usually encapsulated within a nanostructure together with therapeutic anticancer drug. The mechanism of copper ions is based on a Fenton-like reaction which mediates generation of hydrogen peroxide [126]. For palmitoyl ascorbate, its ascorbate group can be oxidized to ascorbate radical that donates an electron to oxygen, forming superoxide radical and ultimately the tumoricidal H_2O_2 [128]. And the α-TOS is a vitamin E analogue, which can rapidly generate ROS in cells based on the interaction with mitochondrial respiratory complex II and interference of electron transportation chain. Zhang's group reported a positive feedback mesoporous silica NPs (MSNPs) loaded with α-TOS and DOX for ROS responsive drug delivery (Fig. 8B) [127]. In the system, β-cyclodextrin crystalline (β-CD) serving as gatekeepers was anchored on the surface of MSNPs via ROS-cleavable thioketal linker. And adamantane conjugated PEG (AD-PEG) was coated for prolonged circulation time. After cell internalization, in response to insufficient intracellular ROS, only limited pores of MSNPs were open, but simultaneously caused the release of α-TOS. Then additional ROS was generated, finally leading to the break of thioketal linkers accompanied with effective release of DOX. The new ROS triggers also facilitated the production of more α-TOS which further reinforced the positive feedback loop of thioketal linker cleavage. *In vitro* study with 100 μM H_2O_2 incubation demonstrated the system with efficient DOX release profile. The group further conducted the *in vivo* antitumor experiments and it's demonstrated that the MSNPs exhibited more significant antitumor effect in the

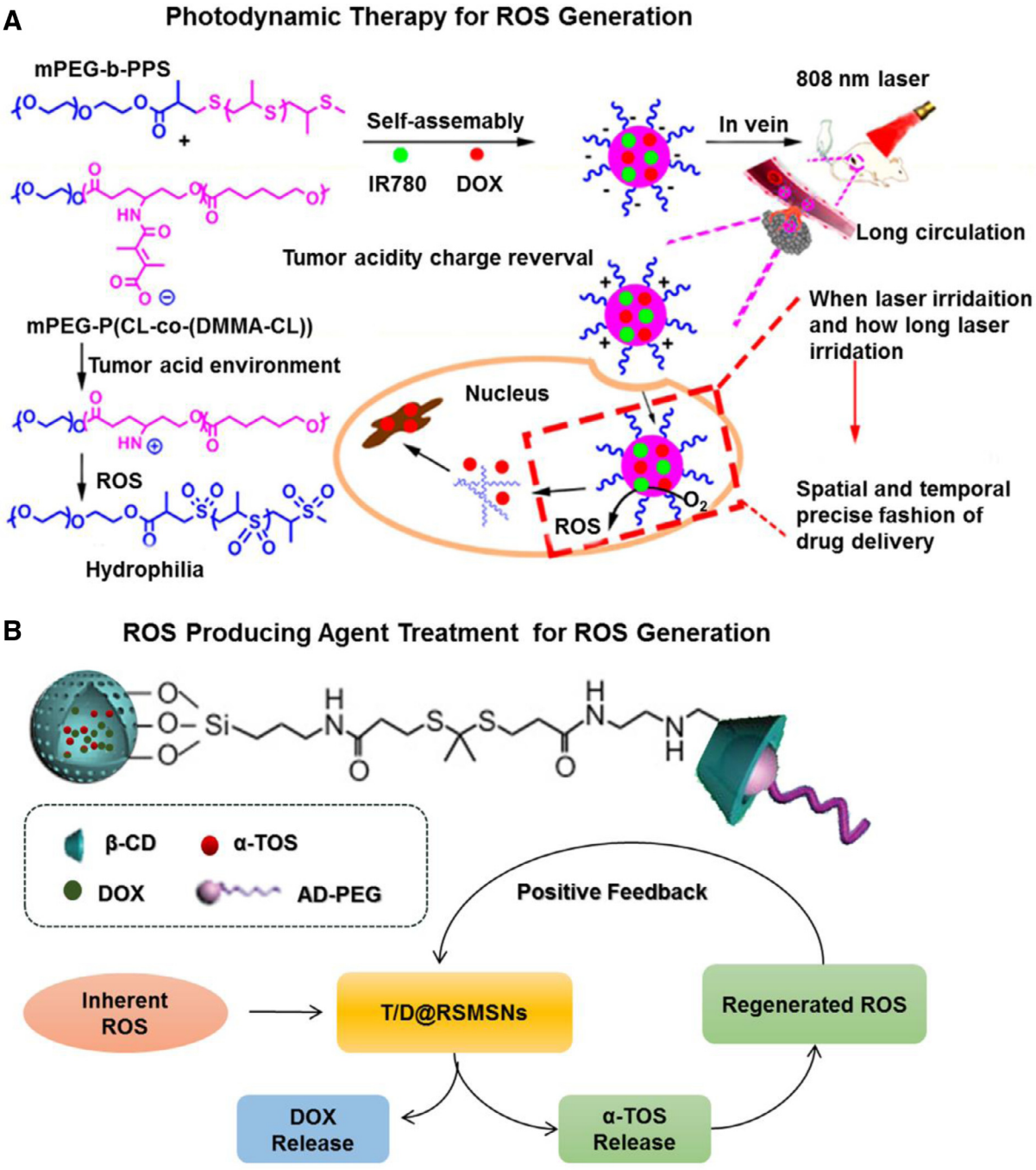

Fig. 8 – ROS responsive drug DDSs. (A) ROS generation based on photodynamic therapy: the construction of Pros-PDC NPs with prolonged circulation time and enhanced cellular internalization, and light-triggered ROS generation and the newly generated ROS activated anticancer drug release of the DOX and IR780 co-loaded Pros-PDC NPs with a spatially and temporally precise profile, adapted from reference (Reproduced with permission from [120]. Copyright 2017 Elsevier). (B) ROS generation based on ROS producing agent administration: structure of T/D@RSMSNs nano-system and its positive feedback mechanism for ROS-responsive self-accelerating drug release (Reproduced with permission from [127]. Copyright 2017 Elsevier). (For interpretation of the references to color in this figure legend, the reader is referred to the web version of this article.)

human breast cancer than the traditional single-DOX loaded ROS-responsive nanocarrier. These nanostructures with ROS-generating-agents possessed great potential to expand the application of H_2O_2 responsive materials.

3.4. *ATP-triggered drug delivery systems*

ATP, known as the "energy currency" in cells, plays a vital role in cellular signaling and metabolism. In the past few years, abundant DDSs based on the sharp concentration difference of ATP between intracellular (1–10 mM) and extracellular (<0.4 mM) environment have been constructed by researchers. In most cases, the ATP content in tumor was much higher than that of the normal tissue, such as murine lymphoma L5178Y cells and mouse leukemia L 1210 [129]. However, the ATP level in hepatoma 3924A cells of rat was decreased to 43% of the normal liver concentration [130,131]. This indicates ATP-triggered DDSs were not suitable for hepatoma. For other tumors, this stimuli was usually applied in tuning the intracellular and extracellular "stability" of the carriers for enhanced blood circulation and on-demand drug release. There are mainly four types of modules adopted in these systems up to now: 1) ATP aptamers having a strong affinity with ATP; 2) phenylboronic acid-sugar-functional polymers; 3) ATP consumer enzymes. 4) Zinc-dipicolylamine (TDPA-Zn^{2+}). Among them, ATP aptamers gained most popularity due to their relatively short sequences (~30 bases), simple modification and specific response.

3.4.1. *ATP aptamers-based drug delivery systems*

Screened from a large pool of random ssDNA sequences *in vitro*, ATP aptamers are single strand DNA (ssDNA) with high binding affinity against ATP [132-134]. ATP aptamers can bind with single strand nucleotides forming DNA duplex via complementary base pairing. The DNA duplex has been incorporated into various drug carriers, such as poly(ethylenimine) (PEI) [135,136], MSNPs [137], MOFs [138], nanogel [139], liposome [140], nanosheet [141,142], microcapsules [143–145], and etc.

Unique physical and chemical features of ATP aptamers include rich "GC" pairs and negatively charged surfaces, allowing multiple attachment of anticancer agents and cationic polymers. This provides new insight for development of co-delivery systems [135,136]. DOX and siRNA co-delivery system was reported. DOX was incorporated into the GC-rich DNA duplexes, and then, cationic PEI was employed as a carrier to condense negatively charged DOX duplexes and miRNA, which finally obtained a ternary nanocomplex denoted as PEI/DOX-Duplex/siRNA. The combination therapy of chemotherapeutic agents and oligonucleotide-based genes could induce synergistic effects and significantly improve the efficiency of cancer treatment. Meanwhile, ATP aptamers can also be used as gatekeepers to regulate the release of drugs from porous materials, such as MSNPs [137] and MOFs [138]. Chen et al. fabricated a MOF nanoparticle composed of Zr^{4+} and triphenyl dicarboxylic acid (TPDC) [138]. The organic composite was terminated with amino group, and transformed into azido for dibenzo cyclooctyne (DBCO) functionalized ATP aptamer modification. The AS1411 aptamers with specific recognition of receptors on cancer cell membrane were further attached to form DNA duplex for pores blockage. ATP treatment led to the "unblock" of the pores via formation of ATP/ATP aptamer duplexes and achieved stimulated drug release. In addition, the DNA coated MPFs revealed selective and effective cytotoxicity toward MDA-MB-231 breast cancer cells as compared to normal MCF-10A epithelial breast cells.

Gu's group reported a novel nanogel composed of DNA duplex as a core and HA as a shell for ATP-responsive drug release (Fig. 9A) [139]. Similarly, DNA duplex rich in "GC" pairs allowed the incorporation of DOX which can be released via an effective structural change to aptamer/ATP complexes. To neutralize the negative charge of the DNA duplex, positively charged protamine (a cell-penetrating peptide) was applied to form a cationic core complex, onto which anionic HA was coated as a shell. The HA coating not only served as a protective shell but also was active ligand of overexpressed receptors on the cancer cell membrane, such as CD44 and RHAMM. In addition, HA is the substrate of the enzyme hyaluronidase which is rich in tumor environment, especially tumor matrices and cancer cellular endocytic vesicles, leading to the degradation of HA shell to facilitate intracellular delivery. *In vitro* and *in vivo* studies demonstrated that this system showed a high selectivity between intracellular and extracellular environment, leading to an enhanced therapeutic effect of breast cancer.

With the purpose of further accelerating drug release from the DNA duplexes, the same group encapsulated extrinsically supplemented ATP in liposomes forming a co-delivery system [140]. To enhance endosomal escape and nuclear targeting, the negative charged duplex loaded with DOX was also coated by positively charged protamine peptide, and then encapsulated in another liposome. Specially, fusogenic dioleoyl phosphatidylethanolamine (DOPE) with pH responsiveness (pH 6.0) was integrated into the liposome membrane through which the fusion of these two liposomes were able to be triggered by acidity of endocytic vesicles. And for active targeting, a cell-penetrating peptide (CPP, R6H4) was modified on the liposome membrane. Thus, the accelerating release of DOX was achieved in cytosol. In MCF-7 cancer xenograft nude mice, the platform with additional ATP administration showed remarkably higher inhibition effects toward tumor growth than free DOX and the control group without exogenous ATP.

In 2015, 2D nanosheets were also applied as carries for ATP responsive systems by Gu et al. They designed a DNA-graphene hybrid nanoaggregate where DOX was attached onto graphene oxide (GO) efficiently via pi stacking function [146]. The ATP aptamer served as hybrid crosslinkers between two DNA-GO-sheets, resulting in the assembly of the DNA-GO-sheets and formation of the multilayer-structural DNA-GO nanoaggregates. Triggered by ATP, the formation of the ATP/ATP aptamer complexes causes the dissociation of the nanoaggregates to facilitate the DOX release. Specially in 2017, Li et al. reported a new class of 2D materials, MoS_2 nanosheets, for ATP responsive drug delivery [142]. To tackle the functional resistance of MoS_2, the sulfur atomic defect sites on its exfoliated surface were utilized [142,147], where sulfur atom-terminated DNA molecules were anchored. Similar to DNA-GO-nanosheets mentioned above, DNA oligonucleotides modified MoS_2 nanosheets could further link with ATP aptamers and quickly self-assembled

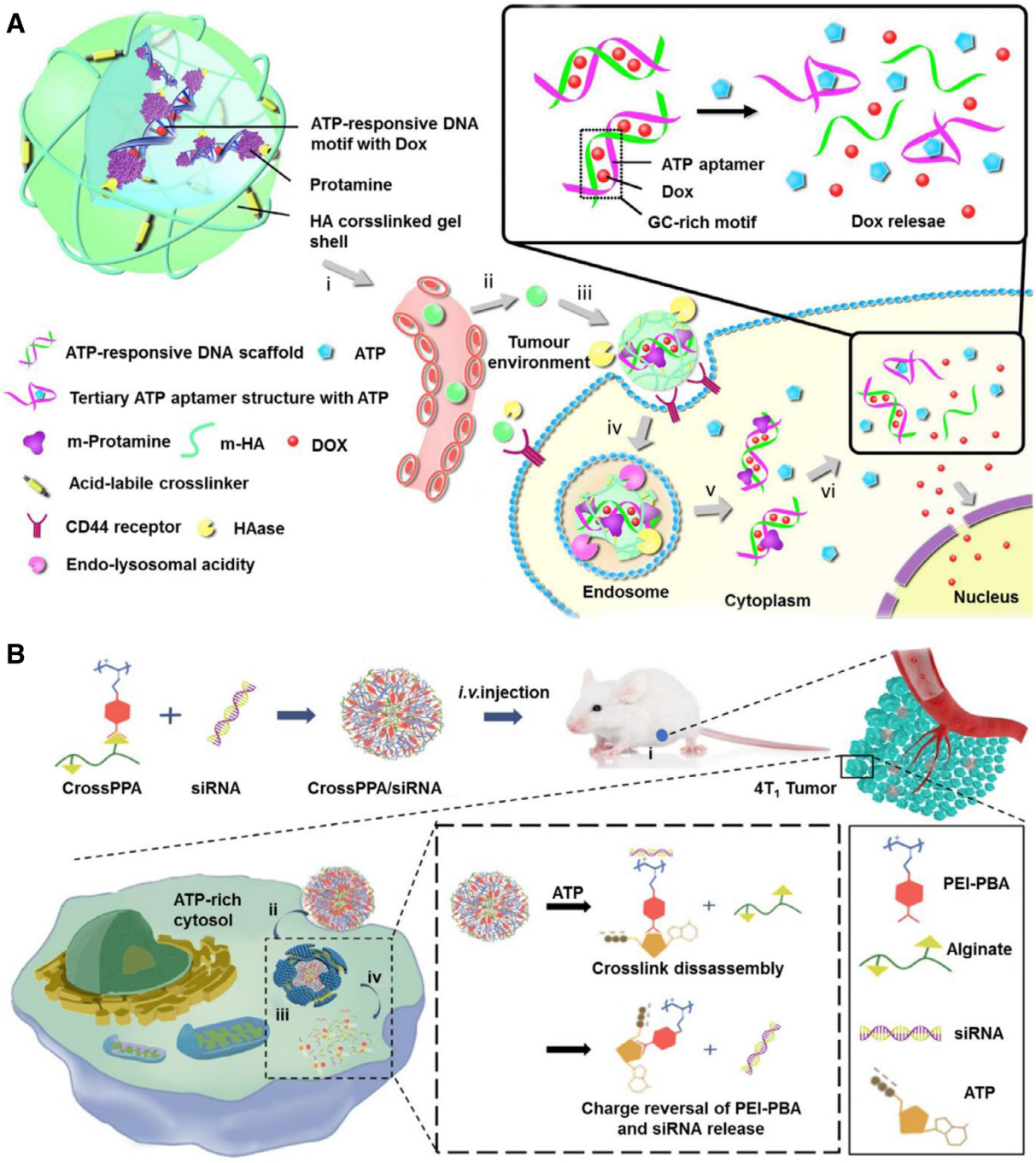

Fig. 9 – ATP triggered drug release. (A) Nanogel composed of an ATP-responsive DNA motif, protamine and a HA crosslinked shell for cellular delivery of DOX (Reproduced with permission from [139]. Copyright 2014 Springer Nature). (B) ATP-responsive charge reversal crosslinked polyplex for tumor-targeted siRNA delivery (Reproduced with permission from [148]. Copyright 2018 Ivyspring).

into a multilayer structure, which was responsive to ATP via dissociation.

Using $CaCO_3$ or SiO_2 template particles as cores, aptamer-functional polymers can also be assembled layer by layer as the shell forming core-shell structures [143–145]. The core could be dissolved by EDTA and followed to form microcapsules. In these systems, aptamers served as bridged linkers of the multilayer shell, which also triggered the release of drug. Liao's team synthesized different types of stimuli-responsive aptamer microcapsules as carriers for different payloads [143]. They investigated the drug release profile of the DDSs loaded with dextran, quantum dots or myeloperoxidase. The results demonstrated that ATP efficiently triggered the formation of aptamer-ATP complexes and resulted in a decomposition to release the various loads. Due to the wide array of sequence-specific vectors, it is also possible to design synthetic materials of other ligands with different payload carriers whose dissociations depend on aptamer-ligand complexes formation.

3.4.2. *Phenylboronic acid-sugar-functional polymers*

In the development of ATP responsive DDSs, the reversible ester formation of phenylboronic acid (PBA) with diols has attracted more and more attention [148–152]. ATP with a cis-diol moiety in its ribose ring, can compete with other diols resulting in the formation of PBA-ATP with better thermodynamic stability. Meanwhile, PBA can be used as a targeting ligand for its specifical binding to sialylated epitopes overexpressed on the surface of tumors [153]. Furthermore, with pH value below its pK_a, PBA undergoes charge transition from neutral to positive and polar change from hydrophobic to hydrophilic [154]. These features make PBA-based materials as excellent carriers for pH or/and ATP responsive drug delivery.

In a study by Naito et al., a PBA-functionalized polyion complex micelle was designed where therapeutic agent "siRNA" was encapsulated in the micelles through the binding between its ribose and PBA [151]. In their work, cationic poly (ethylene glycol)-block-poly (L-lysine) (PEG-b-PLys) polymers were first prepared terminated with lysine residues, of which the amino groups were functionalized with 3-fluoro-4-carboxyphenyl boronic acid (FPBA) based on carbodiimide chemistry. The cationic polymers were then interacted with siRNA and assembled into micelle. The obtained micelle was remarkably stable due to siRNA cross-linking at concentration level of extracellular ATP, but it was disrupted at intracellular level of ATP for the formation of PBA-ATP complex, accompanied with the release of the siRNA. Kim et al. synthesized PBA-galactose grafted poly(ethylenimine) (PEI) copolymers for the delivery of anti-angiogenic gene (pDNA) [152]. Cationic poly(ethylenimine) (PEI) chains were modified with PBA and galactose (GA), respectively, at both terminals, and the obtained two polymers formed boronic ester bonds via the binding of PBA and diols of GA. Then the anionic gene was attached onto cationic PBA-galactose modified PEI copolymers via PBA-diol and electrostatic binding. Further, PEG was introduced to increase the blood circulation time. Specially, the binding between PBA, siRNA, and galactose can be disrupted by either acidic endosomal pH or intracellular ATP. Effective release of pDNA was demonstrated at acidic pH or in the presence of intracellular concentration of ATP (5 mM). *In vivo* studies in MCF-7-xenografted mice revealed that the prepared PBA-PEG-CrossPEI copolymers selectively bound to tumor cells with around twice amount of tumor accumulation than PEG-CrossPEI and achieved efficient delivery of pDNA to inhibit tumor growth.

In a recent study by Sun's group, PEI polymers conjugated with PBA were also reported as carriers for the delivery of genes (Fig. 9B) [148]. They leveraged the negative charge feature of ATP in the cytosol of cancer cell to avoid the released anionic siRNA reintegrating with the cationic carriers. In detail, PBA was attached to PEI polymers based on carbodiimide chemistry. The PBA group of the obtained PEI-PBA polymer was bound to diol groups on alginate forming a cationic PEI-PBA-alginate structure (CrossPPA), onto which the anionic siRNA was further attached (CrossPPA/siRNA). After intravenous injection, the CrossPPA/siRNA NPs went through a cascade of four steps: at first the NPs were accumulated at tumor tissue; then PBA groups medicated specific recognition of sialic acid (SA) over-expressed cancer cells for enhanced cellular uptake; and subsequent endosomal escape was achieved; at last, cellular ATP broke up the borate ester bond of the CrossPPA/siRNA complexes resulting in the removal of alginate, furthermore, the anionic ATP reversed the charge of the PEI-PBA polymer from positive to negative which facilitated the siRNA release because of electrostatic repulsion. The negative charge of the PEI-PBA/ATP complexes was capable of avoiding interaction with the released siRNA and following gene silencing. The anti-tumor efficacy was studied in 4T1 tumor-bearing mice. It turned out that the CrossPPA/siRNA NPs exhibited significant inhibition of tumor growth owing to its obvious tumor targeting and high transfection efficiency of siRNA.

3.4.3. *ATP consumer enzyme-based drug delivery systems*

Proteins that need ATP as a cofactor or catalyze ATP hydrolysis would be a valuable clue to find suitable candidates for ATP responsive drug delivery [132]. Chaperone GroEL, with a large cavity to capture denatured proteins, is a typical example from these proteins, reported by Aida and coworkers (Fig. 10A) [155]. The protein is an enzyme for catalyzing ATP hydrolysis to form ADP. In their work, cysteine residues were modified on the protein for further introduction of merocyanine (MC)-Mg^{2+}-MC coordination, finally forming a nanotube (NB) like structure. Drugs were sealed within the tube after conjugation with a guest protein fitting its cavity. ATP triggered a conformational change of the chaperone, which generated an internal mechanical force to break the MC-Mg^{2+}-MC interaction, leading to tube dissociation and drug release. Further introduction of boronic acid as targeting ligand, the chaperone exhibited enhanced cell membrane permeability. Furthermore, the results of biodistribution test demonstrated the platform with preferential accumulation in a tumor tissue (HeLa) over other tissues, except liver tissue, indicating that the protein is a promising nanocarrier for intracellular ATP responsive drug delivery.

In addition to structural conformation change, polymer assembly was reported as another ATP-responsive model by Yan et al. [156]. Inspired by natural ATP protein carrier, a diblock copolymer, poly (ethylene oxide)-b-polymethacrylate (PEO_{45}-b-PHM_{126}), were synthesized as the backbone, onto which, β-CD, serving as macrocyclic pendants, was randomly grafted with short bi-guanidine spacers as bridged linker, forming a pocket-like polymer receptor. The polymer receptor can trap ATP via formation of ATP/polymer complexes. This resulted in ATP concentration-dependent decrease in hydrophilic block volume fraction which was related to the geometry of the copolymer amphiphiles. More interestingly, the ATP/polymer hybrid aggregates reversibly disassembled in response to phosphatase. All the characteristics can offer a new insight into the development of ATP-responsive nanocarriers.

3.4.4. *Zinc-dipicolylamine (TDPA-Zn^{2+})-based drug delivery systems*

Zinc-dipicolylamine analogs (TDPA-Zn^{2+}) provide another strategy for the design of the ATP responsive materials. TDPA-$Zn^{2+}$is capable of forming multivalent coordination

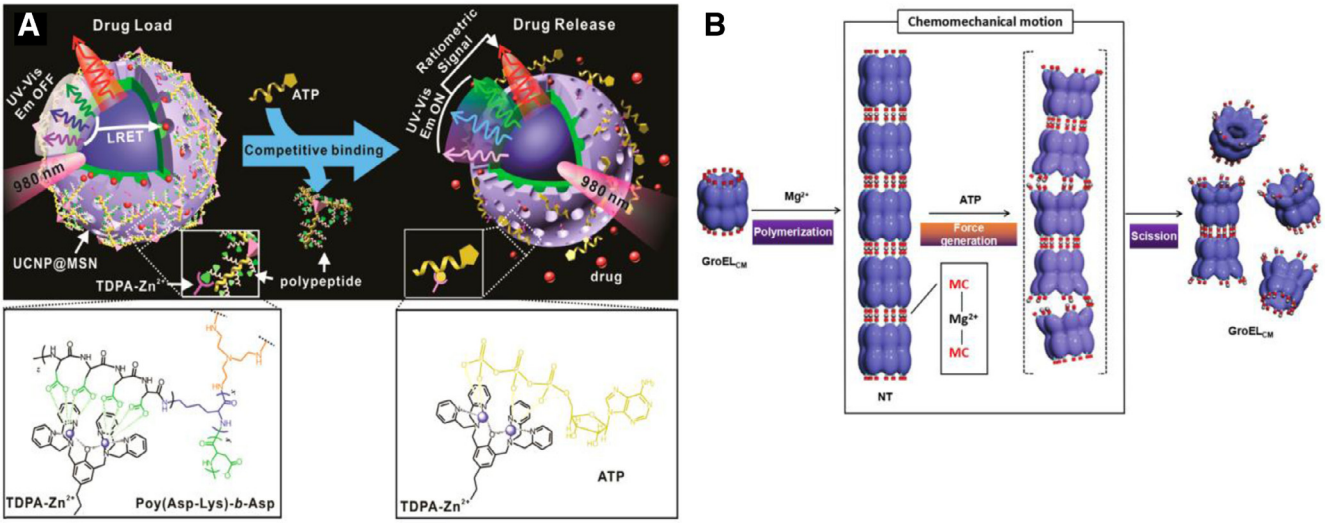

Fig. 10 – ATP triggered drug release. (A) ATP responsive $GroEL_{CM}$ protein based on chemomechanical conformational changes for promotion of intelligent drug release (Reproduced with permission from [155]. Copyright 2013 Springer Nature). (B) TDPA-Zn^{2+}-UCNP@MSNs wrapped with polypeptide for real-time monitoring of ATP-responsive drug release (Reproduced with permission from [157]. Copyright 2015 American Chemical Society). (For interpretation of the references to color in this figure legend, the reader is referred to the web version of this article.)

with polypeptides owing oligo-aspartate moieties and the binding constant was reported to be two magnitude lower than the one with ATP. Based on this, cellular ATP was capable of displacing the polypeptide coordinated with TDPA-Zn^{2+} which facilitated the disconnection of the multivalent interaction. TDPA-Zn^{2+}modified peptides were utilized by Lai et al. as gatekeepers of the mesoporous-silica coated upconversion nanoparticle (UCNP@MSN) for real-time monitoring of ATP responsive drug delivery (Fig. 10B) [157]. The UCNP@MSNs had distinct emission peaks present in UV to NIR region with excitation at 980 nm. The multivalent coordination interactions among UCNP shell, peptide, and TDPA-Zn^{2+} resulted in the quenching of UCNP emission in UV–visible range while retaining their strong NIR emission. Specially, the entrapped model drugs like DOX could lead to the occurrence of luminescence resonance energy transfer (LRET) from the UCNPs (donor) to the loaded drugs (acceptor) in UV-visible range. In tumor microenvironment, cellular upregulated ATP competed with polypeptides, and due to its higher binding affinity, the polypeptides were removed from the TDPA-Zn^{2+}metal complex resulting in the breaking of the multivalent interactions. This accompanied with efficient drug release and subsequent diminishing of LRET signals together with the enhancement of the UV–Vis emission of UCNPs. Thus, monitoring changes in the ratio of LRET and UV–Vis emission could track the drug release behavior from the pores in real time.

3.5. *Enzyme-triggered drug delivery systems*

The pathology of many diseases, such as inflammation, infection, and cancer are associated with elevating concentrations of several enzymes. For example, intracellular legumain and cathepsin were found overexpressed in various tumors including gastric cancer [158], breast cancer [159,160] and colorectal cancer [161,162]. Some extracellular enzymes such as matrix metalloproteinases (MMPs) and hyaluronidases (HAs) were upregulated in almost all types of tumors [163,164]. Based on the biochemical abnormality, a variety of DDSs have been developed by incorporating specific moieties (enzymatic substrates) that can be recognized and degraded by overexpressed enzymes. The intracellular overexpressed enzymes were excellent triggers for controlled drug release within tumor cells. Meanwhile, these extracellular upregulated enzymes can serve as triggers for size shrinkage and surface ligand exposure to obtain enhanced penetration into deep tumors and cellular internalization. In this section, the recent reported enzyme responsive carriers such as legumain, cathepsin, metalloproteinases and other enzymes were summarized.

3.5.1. *Legumain*

Legumain is an asparaginyl endopeptidase upregulated in the lysomes of several cancer cells [165]. It has highly strict specificity to cleave linkers presenting asparagine or aspartic acid residues [166]. In view of this feature, legumain degradable peptides were synthesized for on-controlled cellular drug delivery. And the terminal carboxyl group of the peptides can be further conjugated to antitumor drugs through amide bond formulation. Zhang et al. reported a legumain cleavable micelle, based on AANL (alanine-alanine-asparagine-leucine) peptides as linkers for intracellular delivery of DOX [167]. The linkers conjugated 4-arm PEG and DOX, forming a prodrug copolymer (4-arm PEG-AANL-DOX) with the ability to self-assemble into micelles in aqueous solution. The micelles with a prolonged circulation time could accumulate in tumor tissue and achieve legumain responsive drug release. Furthermore, *in vivo* studies on nude mice bearing MDA-MB-435 tumors revealed that the designed DDSs had a comparable anticancer efficacy with the free DOX but

decreased DOX-related toxicities to normal tissues. However, such NPs also targeted to normal cells with low expression of inactive legumain, leading to a decreased therapeutic efficiency. To evade undesired normal cellular internalization, targeting moieties are required for improvement of the overall targeting efficiency. Nan's group prepared a legumain sensitive HA nanogel where HA served as the targeting agent [166]. The legumain responsiveness was achieved via AANL peptide bridges, onto which, HA and DOX were conjugated. With the introduction of HA, the nanogel could achieve specific binding with CD44 receptors overexpressed on cancer cells. DOX in the cancer cells was more remarkable than that in the normal cells. The group further evaluated the therapeutic efficacy of the developed nanogel in a lung cancer mice model. The results turned out that the nanogel treated group showed no significant ($P < 0.05$) changes in tumor size and all mice survived for 40 d while free DOX suppressed the tumor growth for only up to 20 d with systemic DOX toxicity in both liver and kidney.

Also, immune cell membranes with tumor homing feature were also leveraged as targeting function for legumain activated drug delivery. Li's group reported legumain cleavable NPs encapsulated within $Ly6c^+$ inflammatory monocytes for lung metastasis treatment [168]. In this case, legumain substrate AANK (alanine-alanine-asparagine-lysine) peptide acted as the legumain responsive linkers where cytotoxic mertansine and poly (styrene-co-maleic anhydride) (SMA) were further attached. The obtained NPs were denoted as SMNs. This biomimetic platform underwent a two-stage drug release process. The first stage was that the responsive differentiation of monocytes into macrophages at lung metastasis site resulted in the breaking of the monocyte membrane to promote the release of the intelligent SMNs. The second stage was that the cellular legumain triggered the cleavage of AANK peptides and achieved drug release at the desired site. *In vivo* studies on lung metastases mice model demonstrated that the SMNs significantly improved the delivery of drugs to lung metastases and penetration into deep metastatic tumors, thus producing a 77.8% inhibition of lung metastases.

By Li's group, macrophages were developed as scaffolds for insertion of legumain and redox responsive moieties to target lung metastasis (Fig. 11A) [169]. In their work, propeptide melittin (legM) with AAN (alanine-alanine-asparagine) peptides served as the legumain responsive linkers and further conjugated with DMPE-PEG to form the DMPE-PEG-legM conjugate while disulfide bridges with redox responsivity were conjugated with cytotoxic DM4 and DMPE to form the prodrug DMPE-PEG-S-S-DM4. DMPE was the abbreviation of 1, 2-dimyristoyl-sn-glycero-3-phosphor ethanolamine-N–methoxy group which facilitated the direct insertion of functional moieties onto the membrane of macrophages. The obtained legM- and DM4-loaded macrophages (LD-MDS) first achieved tumor homing at lung metastasis site and the overexpressed legumain triggered the cleavage of AAN linkers causing the formation of the active melittin, which promoted the responsive transformation of DM4-loaded exosome-like nano-vehicles (DENs). The released DENs were then internalized by metastatic cancer cells and led to significant cell apoptosis at redox environment. It's interesting that the damaged cancer cells were able to achieve secondary release of the DENs and free drugs to kill the neighboring cancer cells. The results of *in vivo* studies on lung metastatic breast cancer revealed that the prepared NPs exhibited a remarkable reduction of the average number of lung metastatic nodules, which was only 10.5%, 11.4% and 19.0% of the nodules observed in the free macrophage, legM-MDS and DM4-MDS groups, respectively, indicating a significant inhibition of the lung metastasis.

3.5.2. *Cathepsin B*

Cathepsin B (C_B), a late endosomal and lysosomal cysteine protease, plays a major role in the progression of human tumors [170]. Taking advantage of this specificity, several C_B-cleavable peptide sequences were developed such as VC (Valine-Citrulline) peptides, FRRG (Phenylalanine-Arginine-Arginine-Glycine) peptides and GFLG (Glycine-Phenylalanine-Leucine-Glycine) peptides [170–173]. Yu and colleagues designed a novel and safe micellar drug carrier for DOX delivery, which was made use of VC dipeptide conjugating hydrophilic mPEG and hydrophobic stearic segment [170]. The micelles had almost no cytotoxicity against Bx PC-3 cells, but showed no obvious increase of accumulative drug release ratio *in vitro* in the presence of C_B. Thus, further exploration of the micellar system is needed for a satisfactory drug release behavior. Specially, in a recent study by Zhang et al., a novel type of amide bond-bearing cathepsin B-sensitive gemcitabine (GEM) prodrugs was reported, where the prodrug could *in situ* covalently target circulating albumin and then made a hitchhike to the tumor [173]. Such a sensitive linker was obtained via the conjugation of 6-maleimidocaproicacid and the amine group of gemcitabine [173]. The group confirmed that various cancer cells overexpressed with C_B, including HT-29, human breast adenocarcinoma (MDA-MB-231), human breast adenocarcinoma (MCF7) and human lung carcinoma (A549), resulting in successful prodrug activity in these tumor cells. In detail, *in vivo* albumin was capable of binding with the maleimide groups of the linker, thus carrying the prodrugs to these tumor [173]. Then triggered by the tumor overexpressed cathepsin B and acidic microenvironment, the system exhibited accelerated release of gemcitabine due to the degradation of amide-containing linker [173]. In addition, the NPs showed successful tumor-targeting ability and enhanced therapeutic efficiency in human colon adenocarcinoma (HT-29) tumor-bearing mice.

GPLG is the most attractive polypeptide for the construction of C_B-responsive drug delivery carrier. It's proved that C_B shows the highest activity at a pH between 5 and 6 [174,175]. Therefore, the enzymolysis of GFLG peptide will be inhibited in blood circulation, further prolonging circulation time of GPLG-based carriers. Cheng et al. leveraged GFLG-containing multifunctional rotaxane structure as gatekeepers of MSNs for C_B responsive drug delivery [172]. The authors demonstrated that 80% of the loaded DOX were released at pH 5.0 in the presence of C_B. Luo et al. reported another C_B specific cleavable platform where GPLG peptides were conjugated with PTX and further attached to PEGylated peptide dendrimer. The negative charged nano-formulation, which integrated the advantages of peptide dendrimer macromolecules, PEG modification, nanoscale

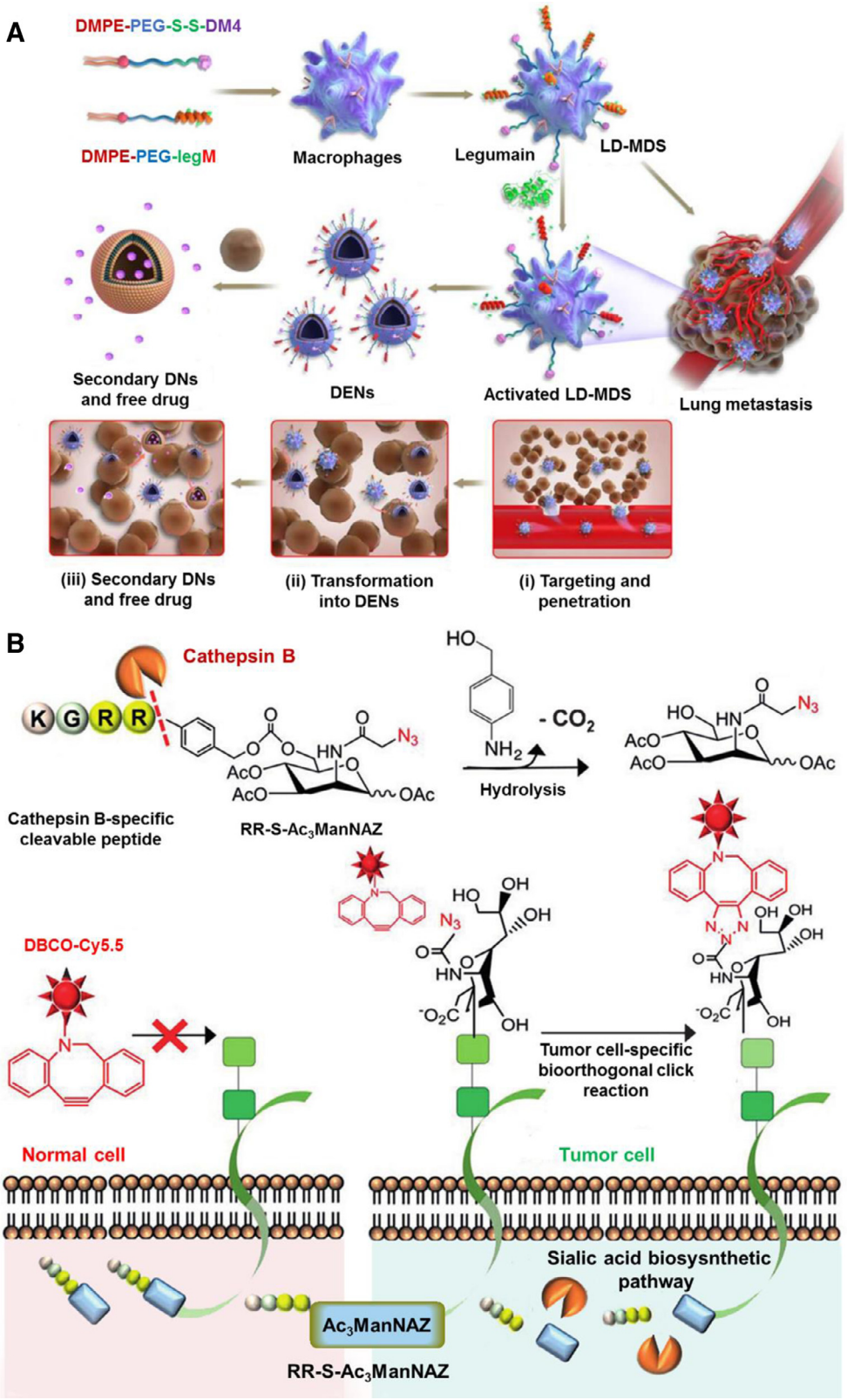

Fig. 11 – Enzyme responsive drug delivery platform. (A) Legumain specific cleavable bioinspired macrophage delivery system for treatment of lung metastasis (Reproduced with permission from [169]. Copyright 2018 American Chemical Society). (B) Cathepsin B-specific cleavable production of Ac_3ManNAz for exogenous generation of chemical receptor on the membrane of cancer cell where specific bioorthogonal click molecule DBCO-Cy5.5 could be actively bound (Reproduced with permission from [176]. Copyright 2016 Wiley-VCH). (For interpretation of the references to color in this figure legend, the reader is referred to the web version of this article.)

system and enzyme-sensitive linker, was expected to achieve overall optimal therapeutic efficiency for PTX delivery. Kim's group reported C_B-specific cleavable KGRR (lysine-glycine-arginine-arginine) peptide caged metabolic precursors for exogenous generation of chemical receptors on cancer cell membrane (Fig. 11B) [176]. The major components of the metabolic precursors included spacer linker of paminobenzyl-oxycarbonyl (S), C_B-cleavable KGRR peptide and the metabolic precursor of triacetylated N-azidoacetyl-d-mannosamine (Ac3ManNAz), leading to the formation of RR-S-Ac3ManNAz. At tumor microenvironment, C_B triggered the cleavage of the KGRR peptide linkers producing RR-S-Ac3ManNAz which was then hydrolyzed to active Ac3ManNAz. Based on metabolic glycol-engineering, the Ac3ManNAz generated unnatural glycans (exogenous chemical receptors) with azide groups (N_3) on the specific cancer cells, which could be targeted with bioorthogonal click-molecule-conjugated NPs like dibenzocyclooctyne (DBCO) via click chemistry. Furthermore, confocal microscopy fluorescence imaging demonstrated the successful generation of the chemical receptors on HT-29 cancer cells as well as the efficient binding of DBCO. This novel system sheds new light on the solution of insufficient expressing receptors on cancer cells.

3.5.3. *Combination of metalloproteinases and Cathepsin B*

Interestingly, Ji et al. constructed a dual enzymatic gemcitabine delivery system for pancreatic cancer therapy [171]. Their research was mainly based on the feature that both matrix metalloproteinases (MMPs, extracellular enzyme) and Cathepsin B (C_B, intracellular enzyme) are up-regulated in several cancers. The system exploited CdSe/ZnS QDs as nano-vectors where RGD was decorated for cell internalization. To prolong blood circulation, PEG shied was linked to the nano-vectors through MMPs cleavable peptide sequence (GGPLGVRGK-NH_2). Similarly, gemcitabine was conjugated via C_B substrate peptide GFLG. In the process of systemic circulation, the PEGylated vectors accumulated in tumor tissue based on EPR effects at first. Then in the presence of extracellular overexpressed MMPs, PEG shied was removed and resulted in the exposure of targeting ligand-RGD-for the enhancement of cancer cell internalization. After cellular uptake, GEM would be released by the trigger of up-regulated CB in the cell. Both *in vitro* and *in vivo* study demonstrated that the GEM nano-vectors had prolonged circulation time, enhanced cellular internalization and efficient drug release.

3.5.4. *Other lysosomal enzymes for controlled drug delivery*

Additional lysosomal enzymes including esterase, amylases, β-D-galactosidase and amidases are also reported as triggers for intracellular controlled drug delivery [177–179]. Awino et al. designed therapeutic nucleic acid-functionalized nanocapsule with esterase responsiveness which provided a potential nanocapsule for co-delivery of small molecule drugs and therapeutic nucleic acids alike [179]. An esterified diazido cross-linker with esterase specific cleavage responsiveness was first linked with an alkyne-terminated surfactant via click chemistry while the remaining alkyne groups provided attachment for thiolated DNA molecules. It's interesting that the nanocapsules were assembled from nucleic acid ligands via stepwise thiolyne chemistry under ultra violet light irradiation. And therapeutic DNAzyme, a short nucleic acids sequence, was further functionalized on the nanoscale scaffold, which was able to cleave transcription factor associated mRNA in inflammation pathways. Besides, the cavity of the assembled nucleic acid ligands provided accommodation for small therapeutic molecules. The degradation of the nanocapsules was triggered by cellular upregulated esterase at tumor site, finally resulting in the release of the encapsulated molecules and the therapeutic Enzymes. Further by systematical synthesis of different chemically unique crosslinkers, such formulations could be applied in the development of DDS responsive to a variety of different enzymes.

Bernard's et al. designed nonmetric silica mesoporous particles capped with "Saccharides" for amylase or β-D-galactosidase triggered drug delivery [177]. It's noteworthy that the author employed hydrolyzed starch derivatives with different hydrolysis degree and lactose to control the release profile. It was found that drug release profile was both enzyme-dependent and hydrolysis degree-relevant, providing us with a novel strategy to design well-controlled DDSs. Based on amidases, the same group developed another ε-poly-L-lysine capped MSNs for intracellular-controlled release [178]. They exploited two different methods to anchor ε-poly-L-lysine chains onto the mesoporous surface. One was by means of the amino groups in the side chains of the lysine amino acids and the other was through the polymer's carboxyl-terminal group. The author speculated that the random grafting of the peptide chains contributed to a faster drug release profile.

3.6. *Other mediators*

Inflammation has been characterized as one of the hallmarks of cancer [180]. Inflammation was linked with many types of cancer including bladder, cervical, gastric, intestinal, esophageal, ovarian, prostate and thyroid cancer [111]. In some tumor types, the inflammation is presented before a malignant change occurs, while in other types, an oncogenic change induces an inflammatory microenvironment that promotes the development of tumors [111]. Cancer cells produce pro-inflammatory cytokines, chemokine's and growth factors. With recruitment of these inflammatory mediators, vast inflammatory cells migrate to the tumor site and undergo activation, inducing the secretion of an assorted array of cytokines including tumor necrosis factor (TNF), interleukin-1β (IL-1β) and interleukin-6 (IL-6), which supports tumor survival and proliferation [181]. Unique features of these immune cells include tumor homing and secretion activated by inflammatory mediators, opening a new area for optimization of the carrier accumulation, cellular internalization and efficient drug/NPs release. So far, various immune cells, such as neutrophils [182–184], monocytes [185,186], macrophages [187–189], lymphocyte [190–194] and even platelets [195,196], have been applied in cancer therapy. Some immune cell membrane medicated NPs are summarized in Table 3. In these systems, therapeutic molecules are generally encapsulated in the NPs, and then integrated to immune cells based on covalent attachment, monovalent absorption, endocytosis process or specific antibody-antigen interactions [197,198].

Table 3 – Immune cell membrane-mediated NPs for tumor therapy.

Cell type	Size (μm)	Loaded NPs	Targeting mechanism	Drug release mechanism	Pathological model
Neutrophils [182]	10–12	Liposomes (PTX)	Inflammation factors (IF)	IF induced neutrophil extracellular traps (NETs) release	G422 glioma cancer cells
Monocytes [185]	~25	PLGA (DOX)	Adhesion molecules	Enzyme degradation	Metastatic MCF-7 breast cancer cells
Macrophages [187]	~25	Liposomes (Emtansine)	Adhesion molecules	pH-sensitive liposome destruction	Metastatic 4T1 breast tumor mode
Lymphocyte [193]	6–12	Lipid NPs (Interleukins)	Homing to tumor site	IF responsive drug release	Melanoma-specific Pmel-1 CD^{8+} T cells
Platelet [196]	2–4	a-PDL1	Immune factors	Inflammatory factor-induced release of platelet-derived microparticles	Post-surgical tumor bearing
Dendritic cell [203]	6–12	PLGA (lysate protein antigens)	Immune recognition	Unclear	Ovarian cancer

Chan's group reported a core-shell type "nano-ghosts" for breast cancer therapy [185]. Here, monocyte membrane was coated onto the surface of DOX-loaded PLGA core to actively target breast tumor which recruited monocytes for proliferation. The targeting mechanism was based on cell adhesion molecules interaction. $\alpha 4\beta 1$ integrin on monocytes can specifically bind to vascular cell adhesion molecules-1 (VCAM-1) overexpressed on breast cell membrane, through which natural accumulation at tumors can be easily achieved. However, this system faced difficulties in functionalization at their surface. In another study by Pastoring et al., a hybrid nanocarrier composed of lipids and monocyte membrane was constructed to delivery albumin for colon adenoma-carcinoma therapy [186]. This hybrid system was expected to integrate the advantages of these two materials, such as functional surface and natural accumulation at tumors, showing great potential for cancer therapy. Fluorophores rhodamine and nitrobenzoxadiazole (NBD) were conjugated to the lipids to investigate whether these two materials were fused into unifying liposomes. The formulation exhibited a reduction of fluorophores emission, indicating the long distance between lipids, suggesting that these two moieties were successfully inserted into monocyte membrane. Unfortunately, the system showed no obvious enhanced tumor accumulation compared with control liposomes which might attribute to the structural imperfection of the monocyte membranes after lipids incorporation.

In 2017, Zhang et al. demonstrated that activated neutrophils were capable of mediating the delivery of therapeutic liposomes loaded with PTX across the blood brain barrier into inflammation sites of postoperative glioma via conformational change [182]. Activated by concentrated inflammatory factors at the targeting site, neutrophils were able to release neutrophil extracellular traps (NETs) together with PTX-containing liposomes to achieve tumor cytotoxicity. Also, platelets were also reported as appropriate carriers for post-surgical cancer therapy (Fig. 12A) [196]. In this case, anti-programmed-death ligand 1 (a-PDL1) was bound to the surface of platelet membrane through bifunctional maleimide linkers. Platelets adhesion lead to the generation of platelet microparticles (PMPs) that contain many molecules with immune functions and the diameter of which ranges from 0.1 to 1.0 μm. Then activated by concentrated inflammatory factors, these PMPs were dissociated from plasma membrane in the form of membrane vesicles and released into the extracellular environment. The binding of a-PDL1 to non-activated platelets was highly stable, while the release of a-PDL1 was significantly promoted on the activation of platelets (Fig. 12B and 12C). In mouse model, triple-negative breast carcinomas or primary melanomas were inhibited, overall mouse survival was significantly prolonged and the risk of cancer regrowth and metastatic spread were reduced. Recently, the group further developed a two-cells-in-one combo system for anti-leukemia therapy (Fig. 12D) [199]. They covalently conjugated a-PDL1-loaded platelets to hematopoietic stem cells (HSC), where the HSC served as the targeting cell with bone marrow (leukemia location site) homing feature, and the platelets were drug carriers with tumor environment responsive drug release property. After intravenous injection of this DDSs into leukemia cells-bearing mice, the two cells combo system migrated to the bone marrow and released a-PDL1 at leukemia site, achieving efficient immune responses and prolonged the survival time of leukemia mouse. However, these cell-based systems might release pro-inflammatory factors or activate systemic T-cell during blood circulation, which remains to be further studied for clinical application.

4. Multistage drug delivery systems

DDSs responsive to single stimulus have been proven effective to overcome one biological barrier during CAPIR process. But each step of the CAPIR cascade might weaken the overall delivery efficiency of the DDSs. Thus, an ideal platform should respond to multi-stimuli for further improvement of the drug delivery.

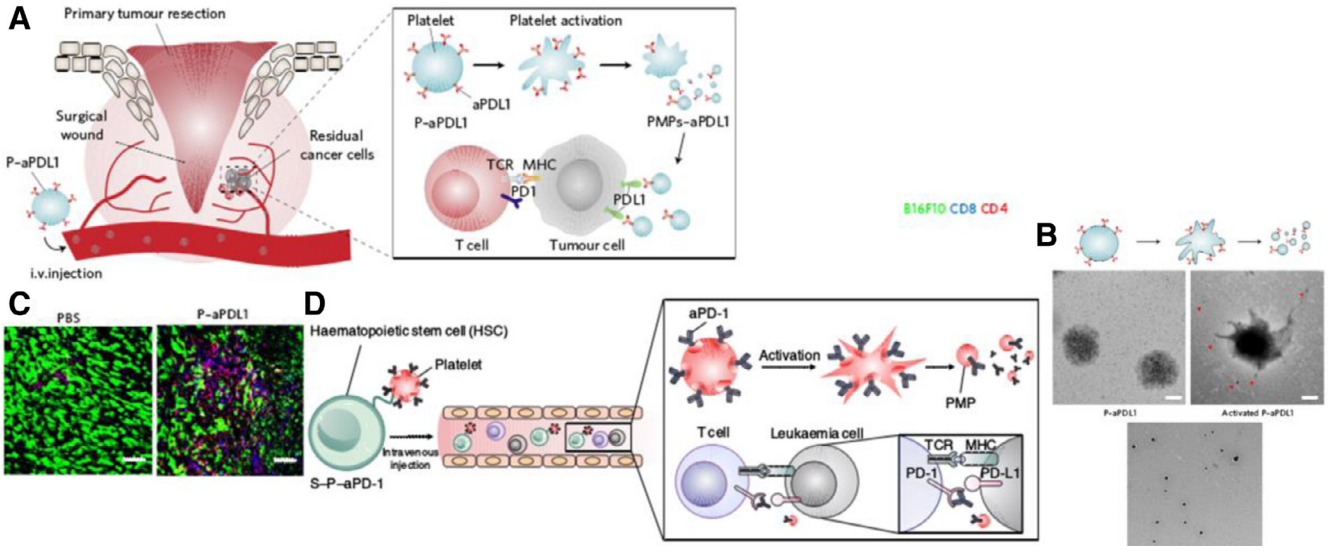

Fig. 12 – Inflammatory mediators activated DDSs. (A) In situ activation of the platelets-based DDSs medicated by inflammatory factors facilitated the release of anti-PDL1 (aPDL1) and cytokines (Reproduced with permission from [196]. Copyright 2017, Springer Nature). (B) TEM images of P-aPDL1 before (left) and after (middle and right) activation (Reproduced with permission from [196]. Copyright 2017, Springer Nature). The red arrowheads refer to the released PMPs from the platelet. (C) Immunofluorescence images of residual tumors showed CD^{4+} and CD^{8+} T cells infiltration. A higher infiltration of T-cells indicates a stronger immune response with a positive correlation to the amount of the released P-aPDL1 (Reproduced with permission from [196]. Copyright 2017, Springer Nature). (D) Integration of hemato-poietic stem cells and platelets for the delivery of anti-PD-1 antibodies to the leukaemia location site (Reproduced with permission from [199]. Copyright 2018, Springer Nature). (For interpretation of the references to color in this figure legend, the reader is referred to the web version of this article.)

Kim et al. developed a multi-staged DDS based on DNA modification for deep penetrating cancer therapy [200]. The formulation combined acidic responsive size shrinkage and ligand exposure into one system. In detail, DOX was loaded on the G-C pairs of DNA duplexes (D_1) and modified on the surface of AuNPs (15 nm), the DOX loaded AuNPs then served as gatekeepers of MSNPs plugging on their pores via another DNA duplexes (D_2). The hybrid MSNPs with a diameter of 150 nm were stable during blood circulation (pH = 7.4). After tumor site accumulation (pH 6.5), the D_2 was hydrolyzed to form a triplex structure, dissociating the AuNPs from the MSNPs pores. The detached AuNPs loaded with DOX possessed a diameter of 15 nm, and could achieve deep penetration into tumor tissues. Internalized by cancer cells (pH 5.0), DOX was released due to the dissociation of the D_1 to form i-motif structures. Studies in MDA-MB-231 cell line and breast tumor bearing mice model demonstrated that the DDSs with tumor specific accumulation, deep penetration into tumor tissue responsive to tumor extracellular pH, and intracellular pH-responsive drug release in a highly sequential manner to achieve high therapeutic efficacy for tumor inhibition. The well-designed nanocarrier with programmed acidic triggered DNA transition provides a typical example of multi-staged responsive DDS design.

Zhang's group designed a pH-/thermal-/GSH-responsive polymer zipper for precise anticancer molecule release [201]. The polymer zipper was polyelectrolyte composites based on multiple salt bridges (pY^-/Gu^+ salt bridges) between cell penetrating peptide-tailed poly(disulfides) with positively charged guanidyl residues (Gu^+/CPD-SS-RGD, RGD is the abbreviation of arginylglycylaspartic acid) and PEG-attached thermosensitive polymers with negatively charged phosphate residues (PY^-/PTPs-PEG) (Fig. 13C). In their work, therapeutic agent was encapsulated in mesoporous silica NPs with positive charge, onto which, anionic hyaluronic acid (HA), cationic Gu^+/CPD-SS-RGD and anionic PY^-/PTP-PEG were assembled forming a sandwich-like structure (Fig. 13C). This formulation underwent a two-stage process for on-demand drug release (Fig. 13A and 13B). The first stage was the detachment of PY^-/PTP-PEG corona due to the combinational trigger of acidic environment and NIR excitation. This resulted in the exposure of the Gu^+/CPD-SS-RGD shell which possessed positive charge and RGD ligand favorite for cellular internalization. The de-shielding of the PEG layer led to size shrinkage of the particles for deep penetration. The second stage was that the positively charged NPs promoted endosomal escape based on "sponge effect" and eventually the intracellular gluthione triggered the cleavage of disulfide bonds and hyaluronidase (HAase) digested the polymer shell, achieving intracellular release of the encapsulated cargoes. The *in vivo* study demonstrated that by controlling the surface states, the nanocarriers showed prolonged blood circulation time, minimized drug leakage in normal tissue, and efficient accumulation and drug release at tumor sites, significantly inhibiting the growth of tumor with slight cytotoxicity to normal tissues.

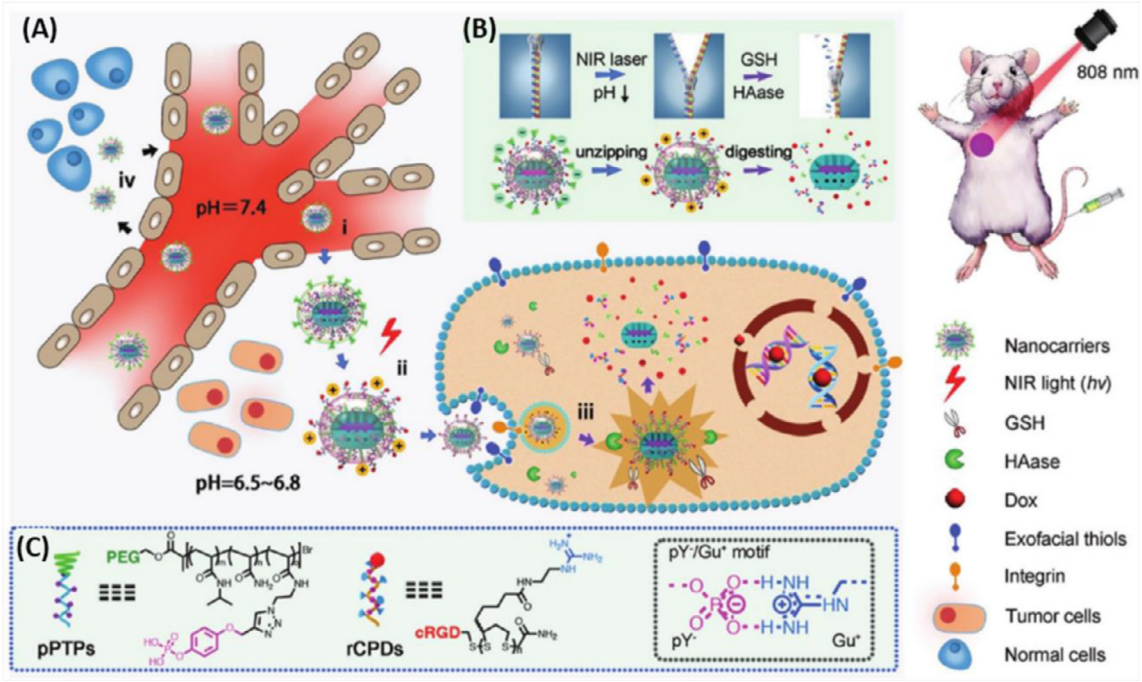

Fig. 13 – Schematic design of smart nanocarriers coated with pH-/thermal-/GSH-responsive polymer zippers for precision anticancer molecular drug delivery (Reproduced with permission from [201]. Copyright 2017 WILEY-VCH). (A) NIR-/pH-guided cellular uptake and GSH/HAase-controlled release *in vivo*. (i) Passive accumulation at tumor sites in the PEG state via the EPR effect; (ii) NIR-/pH-activated surface shift to the Gu^+/CPD-SS-RGD state with positive charge and RGD ligand for selective uptake; (iii) Endosome escape and controlled release by endogenous GSH/HAase; (iv) nonspecific retention and clearance in normal tissues. (B) The surface state variations during drug delivery (the polymer zipper decoding and the sandwich protective shell degradation). (C) The composition of the Gu^+/CPD-SS-RGD and PY^-/PTP-PEG polymer zipper with multiple pY^-/Gu^+ salt bridges. The Gu^+/CPD-SS-RGD was prepared with a cyclic peptide with a sequence of arginine-glycine-aspartic acid (RGD) as an initiator. (For interpretation of the references to color in this figure legend, the reader is referred to the web version of this article.)

5. Conclusions and prospects

There is a wide range of intracellular stimuli-responsive materials having been developed for the delivery of therapeutic compounds. Responding to cellular stimuli such as pH, GSH, ROS, ATP, and enzyme, these intelligent stimuli-responsive nano-devices show a superior anticancer effect and minimized side effect than the conventional formulations. In general, all of the signals mentioned above can serve as triggers for improved stability during circulation and reduced stability for on demand drug release. While extracellular pH and enzymes abnormal in tumor tissue can also tune the NPs size, surface charge and ligand exposure for the optimization of accumulation, penetration and internalization steps. According to previous researches, some of the stimuli like ROS and ATP are insufficient or too slow to induce carrier degradation for on-demand drug release, thus, exogenous stimuli is generated at tumor via direct administration of ATP or PDT/ROS generating agents.

However, the further development for clinical translation is still challenging. The biological process of DDSs was known to be concluded as a CAPIR cascade and each step plays a vital part for the overall anticancer therapeutic efficiency. However, most of the reported carriers were only focused on long blood circulation, enhanced cellular internalization and intelligent cellular drug release. The tumor accumulation and penetration process were ignored, which seemed to incumber the development of smart nanoplatforms. Typical examples of this are PEGylation dilemma and protein corona effect where large particle size and positive charge surface resulted in poor accumulation and penetration separately. The active targeting strategy endows the nanoplatforms with tunable size or charge surface for self-adaptability to different biological environment, providing possible solutions for these dilemmas. But the design of such multi-stage nanoplatforms is still at early stage. Sophisticated design of multi-stage nanoplatforms requires complicated manufacturing process and quality control, becoming a huge obstacle for industrial scale-up. Most of the published papers used implantation animal model to investigate the antitumor effect of these nano-formulations, however, these tumor models cannot accurately represent human tumor in terms of histological characteristics, metastatic pathways, and post-treatment responses. In the future, advanced animal tumor models from genome editing technology and induced by chemicals or virus might possess comparable pathogenesis and pathological features to

evaluate clinical therapeutic potential [202]. Another great challenge is tumor heterogeneity, where the level of cellular stimuli varies in different individuals and pathologic cells. The ambiguity of stimuli concentration within the bodies of patients led to the uncertainty of the responsive behavior and therapeutic efficiency of these nano-formulations for clinical application. To this regard, 3D printing, which allows precise prototyping and manufacturing of dosage forms in numerous textures, sizes and shapes, might provide a solution to produce medications with excellent specifications tailored to the needs of different individuals. Moreover, most of the reported carriers were based on materials without sufficient evidence on safety, biocompatibility and biodegradability, which considerably hinder their clinical translation. Thanks to their advantages, such as prolonged blood circulation, great tumor homing and limited cytotoxicity, the integration of cells and stimuli responsive materials provide a new insight into the demand of CAPIR cascade. Nevertheless, for industrial scale-up, there will be problems with the storage and contamination, as well as the lack of an accepted industrial procedure for preparation of these cell-based carriers. Thus, future studies will require the use of carefully designed experiments and evaluation strategies, and standardization of production process and storage conditions. On the whole, there is still a long way to go for the development and further clinical translation of stimuli-sensitive nanomedicine. It's impractical to design nanocarriers with self-adaptability to all the biological processes. We believe that tumor microenvironment responsive nanomedicines with rational formulations and optimized manufacturing processes will have clinical translational with higher therapeutic effects than the currently commercial drugs.

Conflicts of interest

The authors report no conflicts of interest. The authors alone are responsible for the content and writing of this article.

Acknowledgments

This work was supported by the Huxiang Young Talent Program of Hunan Province (2018RS3005); The Project of Innovation-driven Plan in Central South University (2020CX048); Hunan Provincial Natural Science Foundation of China (2019JJ60071, 2020JJ4680); the Shenghua Yuying Project of Central South University; the Hunan Provincial Postgraduate Research and Innovation Project (CX20190242); and Postgraduate Independent Exploration and Innovation Project of Central South University (2019zzts1017, 2019zzts750), and the Key Research Fund of Hunan Provincial Education Department (18A211).

REFERENCES

[1] Schattling P, Jochum FD, Theato P. Multi-stimuli responsive polymers-the all-in-one talents. Polym Chem 2014;5(1):25–36.
[2] Allen TM. Ligand-targeted therapeutics in anticancer therapy. Nat Rev Cancer 2002;2(10):750–63.
[3] Ju CY, Mo R, Xue J, Zhang L, Zhao ZK, Xue LJ, et al. Sequential intra-intercellular nanoparticle delivery system for deep tumor penetration. Angew Chem Int Ed Engl 2014;53(24):6253–8.
[4] Paliwal SR, Paliwal R, Agrawal GP, Vyas SP. Hyaluronic acid modified pH-sensitive liposomes for targeted intracellular delivery of doxorubicin. J Liposome Res 2016;26(4):276–87.
[5] Chen BL, Dai WB, He B, Zhang H, Wang XQ, Wang YG, et al. Current multistage drug delivery systems based on the tumor microenvironment. Theranostics 2017;7(3):538–58.
[6] Sun QH, Sun XR, Ma XP, Zhou ZX, Jin EL, Zhang B, et al. Integration of nanoassembly functions for an effective delivery cascade for cancer drugs. Adv Mater 2014;26(45):7615–21.
[7] Sun QH, Zhou ZX, Qiu NS, Shen YQ. Rational design of cancer nanomedicine: nanoproperty integration and synchronization. Adv Mater 2017;29(14). doi:10.1002/adma.201606628.
[8] Mishra P, Nayak B, Dey RK. PEGylation in anti-cancer therapy: an overview. Asian J Pharm Sci 2016;11(3):337–48.
[9] Mo R, Gu Z. Tumor microenvironment and intracellular signal-activated nanomaterials for anticancer drug delivery. Mater Today 2016;19(5):274–83.
[10] Xiao HH, Yan LS, Dempsey EM, Song WT, Qi RG, Li WL, et al. Recent progress in polymer-based platinum drug delivery systems. Prog Polym Sci 2018;87:70–106.
[11] Gao ST, Tang GS, Hua DW, Xiong RH, Han JQ, Jiang SH, et al. Stimuli-responsive bio-based polymeric systems and their applications. J Mater Chem B 2019;7(5):709–29.
[12] Chauhan VP, Jain RK. Strategies for advancing cancer nanomedicine. Nat Mater 2013;12(11):958–62.
[13] Sun QH, Radosz M, Shen YQ. Challenges in design of translational nanocarriers. J Control Release 2012;164(2):156–69.
[14] Perrault SD, Walkey C, Jennings T, Fischer HC, Chan WC. Mediating tumor targeting efficiency of nanoparticles through design. Nano Lett 2009;9(5):1909–15.
[15] Cabral H, Matsumoto Y, Mizuno K, Chen Q, Murakami M, Kimura M, et al. Accumulation of sub-100 nm polymeric micelles in poorly permeable tumours depends on size. Nat Nanotechnol 2011;6(12):815–23.
[16] Wang JQ, Mao WW, Lock LL, Tang JB, Sui MH, Sun WL, et al. The role of micelle size in tumor accumulation, penetration, and treatment. ACS Nano 2015;9(7):7195–206.
[17] Dreher MR, Liu W, Michelich CR, Dewhirst MW, Yuan F, Chilkoti A. Tumor vascular permeability, accumulation, and penetration of macromolecular drug carriers. J Natl Cancer Inst 2006;98(5):335–44.
[18] Han M, Huang-Fu MY, Guo WW, Guo NN, Chen JJ, Liu HN, et al. MMP-2-Sensitive HA end-conjugated poly(amidoamine) dendrimers via click reaction to enhance drug penetration into solid tumor. ACS Appl Mater Interfaces 2017;9(49):42459–70.
[19] Li HJ, Du JZ, Du XJ, Xu CF, Sun CY, Wang HX, et al. Stimuli-responsive clustered nanoparticles for improved tumor penetration and therapeutic efficacy. Proc Natl Acad Sci U S A 2016;113(15):4164–9.
[20] Cun XL, Ruan SB, Chen JT, Zhang L, Li JP, He Q, et al. A dual strategy to improve the penetration and treatment of breast cancer by combining shrinking nanoparticles with collagen depletion by losartan. Acta Biomater 2016;31:186–96.
[21] He CB, Hu YP, Yin LC, Tang C, Yin CH. Effects of particle size and surface charge on cellular uptake and biodistribution of polymeric nanoparticles. Biomaterials 2010;31(13):3657–66.
[22] Fischer D, Li YX, Ahlemeyer B, Krieglstein J, Kissel T. In vitro cytotoxicity testing of polycations: influence of polymer structure on cell viability and hemolysis. Biomaterials 2003;24(7):1121–31.

[23] Pack DW, Hoffman AS, Pun S, Stayton PS. Design and development of polymers for gene delivery. Nat Rev Drug Discov 2005;4(7):581–93.
[24] Vermeulen LMP, Brans T, Samal SK, Dubruel P, Demeester J, De Smedt SC, et al. Endosomal size and membrane leakiness influence proton sponge-based rupture of endosomal vesicles. ACS Nano 2018;12(3):2332–45.
[25] Liu D, Yang F, Xiong F, Gu N. The smart drug delivery system and its clinical potential. Theranostics 2016;6(9):1306–23.
[26] Sun CY, Liu Y, Du JZ, Cao ZT, Xu CF, Wang J. Facile generation of tumor-pH-Labile linkage-bridged block copolymers for chemotherapeutic delivery. Angew Chem Int Ed Engl 2016;55(3):1010–14.
[27] Sun CY, Shen S, Xu CF, Li HJ, Liu Y, Cao ZT, et al. Tumor acidity-sensitive polymeric vector for active targeted siRNA delivery. J Am Chem Soc 2015;137(48):15217–24.
[28] Feng T, Ai XZ, An GH, Yang PH, Zhao YL. Charge-convertible carbon dots for imaging-guided drug delivery with enhanced in vivo cancer therapeutic efficiency. ACS Nano 2016;10(4):4410–20.
[29] Zhao W, Li AH, Chen C, Quan FY, Sun L, Zhang AT, et al. Transferrin-decorated, MoS_2-capped hollow mesoporous silica nanospheres as a self- guided chemo-photothermal nanoplatform for controlled drug release and thermotherapy. J Mater Chem B 2017;5:7403–14.
[30] Zhang D, Yang JC, Guan JB, Yang B, Zhang SW, Sun MC, et al. In vivo tailor-made protein corona of a prodrug-based nanoassembly fabricated by redox dual-sensitive paclitaxel prodrug for the superselective treatment of breast cancer. Biomater Sci 2018;6(9):2360–74.
[31] Yang JC, Lv QZ, Wei W, Yang ZT, Dong JJ, Zhang RS, et al. Bioresponsive albumin-conjugated paclitaxel prodrugs for cancer therapy. Drug Deliv 2018;25(1):807–14.
[32] Wei W, Luo C, Yang JC, Sun BJ, Zhao DY, Liu Y, et al. Precisely albumin-hitchhiking tumor cell-activated reduction/oxidation-responsive docetaxel prodrugs for the hyperselective treatment of breast cancer. J Control Release 2018;285:187–99.
[33] Li SH, Zhou SX, Li YC, Li XH, Zhu J, Fan LZ, et al. Exceptionally high payload of the IR780 iodide on folic acid-functionalized graphene quantum dots for targeted photothermal therapy. ACS Appl Mater Interfaces 2017;9(27):22332–41.
[34] Cheng YJ, Zhang AQ, Hu JJ, He F, Zeng X, Zhang XZ. Multifunctional peptide-amphiphile end-capped mesoporous silica nanoparticles for tumor targeting drug delivery. ACS Appl Mater Interfaces 2017;9(3):2093–103.
[35] Liu ZB, Zhao HZ, He LY, Yao Y, Zhou YB, Wu JP, et al. Aptamer density dependent cellular uptake of lipid-capped polymer nanoparticles for polyvalent targeted delivery of vinorelbine to cancer cells. RSC Adv 2015;5(22):16931–9.
[36] Cai SD, Yan JH, Xiong HJ, Liu YF, Peng DM, Liu ZB. Investigations on the interface of nucleic acid aptamers and binding targets. Analyst 2018;143(22):5317–38.
[37] He F, Wen N, Xiao D, Yan J, Xiong H, Cai S, et al. Aptamer based targeted drug delivery systems: current potential and challenges. Curr Med Chem 2018. doi:10.2174/0929867325666181008142831.
[38] Zhong L, Xu L, Liu YY, Li QS, Zhao DY, Li ZB, et al. Transformative hyaluronic acid-based active targeting supramolecular nanoplatform improves long circulation and enhances cellular uptake in cancer therapy. Acta Pharmaceutica Sinica B 2019;9(2):397–409.
[39] Wang ZJ, Guo WL, Kuang X, Hou SS, Liu HZ. Nanopreparations for mitochondria targeting drug delivery system: current strategies and future prospective. Asian J Pharm Sci 2017;12(6):498–508.
[40] Wender PA, Mitchell DJ, Pattabiraman K, Pelkey ET, Steinman L, Rothbard JB. The design, synthesis, and evaluation of molecules that enable or enhance cellular uptake: peptoid molecular transporters. Proc Natl Acad Sci U S A 2000;97(24):13003–8.
[41] Jin EL, Zhang B, Sun XR, Zhou ZX, Ma XP, Sun QH, et al. Acid-active cell-penetrating peptides for in vivo tumor-targeted drug delivery. J Am Chem Soc 2013;135(2):933–40.
[42] Bode SA, Hansen MB, Oerlemans RA, van Hest JC, Lowik DW. Enzyme-activatable cell-penetrating peptides through a minimal side chain modification. Bioconjug Chem 2015;26(5):850–6.
[43] Liu Z, Xiong M, Gong JB, Zhang Y, Bai N, Luo YP, et al. Legumain protease-activated TAT-liposome cargo for targeting tumours and their microenvironment. Nat Commun 2014;5:4280.
[44] Jiang T, Olson ES, Nguyen QT, Roy M, Jennings PA, Tsien RY. Tumor imaging by means of proteolytic activation of cell-penetrating peptides. Proc Natl Acad Sci U S A 2004;101(51):17867–72.
[45] Wang TT, Wang DG, Liu JP, Feng B, Zhou FY, Zhang HW, et al. Acidity-Triggered ligand-presenting nanoparticles to overcome sequential drug delivery barriers to tumors. Nano Lett 2017;17(9):5429–36.
[46] Vaupel P. Tumor microenvironmental physiology and its implications for radiation oncology. Semin Radiat Oncol 2004;14(3):198–206.
[47] Vander Heiden MG, Cantley LC, Thompson CB. Understanding the warburg effect: the metabolic requirements of cell proliferation. Sci Technol Adv Mater 2009;324(5930):1029.
[48] Nilsson C, Kagedal K, Johansson U, Ollinger K. Analysis of cytosolic and lysosomal pH in apoptotic cells by flow cytometry. Methods Cell Sci 2004;25(3–4):185–94.
[49] Engin K, Leeper DB, Cater JR, Thistlethwaite AJ, Tupchong L, McFarlane JD. Extracellular pH distribution in human tumours. Int J Hyperthermia 1995;11(2):211–16.
[50] Ahn B, Lee SG, Yoon HR, Lee JM, Oh HJ, Kim HM, et al. Four-fold channel-nicked human ferritin nanocages for active drug loading and pH-responsive drug release. Angew Chem Int Ed Engl 2018;57(11):2909–13.
[51] Guo X, Wang L, Duval K, Fan J, Zhou SB, Chen Z. Dimeric drug polymeric micelles with acid-active tumor targeting and FRET-traceable drug release. Adv Mater 2018;30(3):1870020.
[52] Zhao Y, Luo Z, Li MH, Qu QY, Ma X, Yu SH, et al. A preloaded amorphous calcium carbonate/doxorubicin@silica nanoreactor for pH-responsive delivery of an anticancer drug. Angew Chem Int Ed Engl 2015;54(3):919–22.
[53] Jin S, Wan JX, Meng LZ, Huang XX, Guo J, Liu L, et al. Biodegradation and toxicity of protease/redox/pH stimuli-responsive PEGlated PMAA nanohydrogels for targeting drug delivery. ACS Appl Mater Interfaces 2015;7(35):19843–52.
[54] Ye DX, Ma YY, Zhao W, Cao HM, Kong JL, Xiong HM, et al. ZnO-based nanoplatforms for labeling and treatment of mouse tumors without detectable toxic side effects. ACS Nano 2016;10(4):4294–300.
[55] Yang X, Grailer JJ, Rowland IJ, Javadi A, Hurley SA, Matson VZ, et al. Multifunctional stable and pH-responsive polymer vesicles formed by heterofunctional triblock copolymer for targeted anticancer drug delivery and ultrasensitive MR imaging. ACS Nano 2010;4(11):6805–17.
[56] Schlossbauer A, Dohmen C, Schaffert D, Wagner E, Bein T. pH-responsive release of acetal-linked melittin from SBA-15 mesoporous silica. Angew Chem Int Ed Engl 2011;50(30):6828–30.

[57] Yu GC, Wu D, Li Y, Zhang ZH, Shao L, Zhou J, et al. A pillar[5]arene-based [2]rotaxane lights up mitochondria. Chem Sci 2016;7(5):3017–24.
[58] Zhuang J, Kuo CH, Chou LY, Liu DY, Weerapana E, Tsung CK. Optimized metal-organic-framework nanospheres for drug delivery: evaluation of small-molecule encapsulation. ACS Nano 2014;8(3):2812–9.
[59] Pang X, Jiang Y, Xiao QC, Leung AW, Hua HY, Xu CS. pH-responsive polymer-drug conjugates: design and progress. J Control Release 2016;222:116–29.
[60] Zheng HQ, Zhang YN, Liu LF, Wan W, Guo P, Nystrom AM, et al. One-pot synthesis of metal-organic frameworks with encapsulated target molecules and their applications for controlled drug delivery. J Am Chem Soc 2016;138(3):962–8.
[61] Kim BJ, Cheong H, Hwang BH, Cha HJ. Mussel-inspired protein nanoparticles containing iron(III)-DOPA complexes for pH-responsive drug delivery. Angew Chem Int Ed Engl 2015;54(25):7318–22.
[62] Sun X, Du RH, Zhang L, Zhang GL, Zheng XJ, Qian JC, et al. A pH-responsive yolk-like nanoplatform for tumor targeted dual-mode magnetic resonance imaging and chemotherapy. ACS Nano 2017;11(7):7049–59.
[63] Kozlovskaya V, Alexander JF, Wang Y, Kuncewicz T, Liu XW, Godin B, et al. Internalization of red blood cell-mimicking hydrogel capsules with pH-triggered shape responses. ACS Nano 2014;8(6):5725–37.
[64] Wang LQ. Preparation and in vitro evaluation of an acidic environment-responsive liposome for paclitaxel tumor targeting. Asian J Pharm Sci 2017;12(5):470–7.
[65] Ma XP, Wang YG, Zhao T, Li Y, Su LC, Wang ZH, et al. Ultra-pH-sensitive nanoprobe library with broad pH tunability and fluorescence emissions. J Am Chem Soc 2014;136(31):11085–92.
[66] Wang YG, Zhou KJ, Huang G, Hensley C, Huang XN, Ma XP, et al. A nanoparticle-based strategy for the imaging of a broad range of tumours by nonlinear amplification of microenvironment signals. Nat Mater 2014;13(2):204–12.
[67] Shi XX, Ma XQ, Hou ML, Gao YE, Bai S, Xiao B, et al. pH-Responsive unimolecular micelles based on amphiphilic star-like copolymers with high drug loading for effective drug delivery and cellular imaging. J Mater Chem B 2017;5(33):6847–59.
[68] Bae Y, Fukushima S, Harada A, Kataoka K. Design of environment-sensitive supramolecular assemblies for intracellular drug delivery: polymeric micelles that are responsive to intracellular pH change. Angew Chem Int Ed Engl 2003;42(38):4640–3.
[69] Lee ES, Na K, Bae YH. Super pH-sensitive multifunctional polymeric micelle. Nano Lett 2005;5(2):325–9.
[70] Luo M, Wang H, Wang ZH, Cai HC, Lu ZG, Li Y, et al. A STING-activating nanovaccine for cancer immunotherapy. Nat Nanotechnol 2017;12(7):648–54.
[71] Yahia-Ammar A, Sierra D, Merola F, Hildebrandt N, Le Guevel X. Self- assembled gold nanoclusters for bright fluorescence imaging and enhanced drug delivery. ACS Nano 2016;10(2):2591–9.
[72] Wyatt LC, Lewis JS, Andreev OA, Reshetnyak YK, Engelman DM. Applications of pHLIP technology for cancer imaging and therapy. Trends Biotechnol 2017;35(7):653–64.
[73] Cheng CJ, Bahal R, Babar IA, Pincus Z, Barrera F, Liu C, et al. MicroRNA silencing for cancer therapy targeted to the tumour microenvironment. Nature 2015;518(7537):107–10.
[74] Kim J, Lee YM, Kang Y, Kim WJ. Tumor-homing, size-tunable clustered nanoparticles for anticancer therapeutics. ACS Nano 2014;8(9):9358–67.
[75] Jia N, Ye YQ, Wang Q, Zhao XL, Hu HY, Chen DW, et al. Preparation and evaluation of poly((L)-histidine) based pH-sensitive micelles for intracellular delivery of doxorubicin against MCF- 7/ADR cells. Asian J Pharm Sci 2017;12(5):433–41.
[76] Wang YH, Song SY, Liu JH, Liu DP, Zhang HJ. ZnO-functionalized upconverting nanotheranostic agent: multi-modality imaging-guided chemotherapy with on-demand drug release triggered by pH. Angew Chem Int Ed Engl 2015;54(2):536–40.
[77] Chen Y, Ye DL, Wu MY, Chen HR, Zhang LL, Shi JL, et al. Break-up of two-dimensional MnO_2 nanosheets promotes ultrasensitive pH-triggered theranostics of cancer. Adv Mater 2014;26(41):7019–26.
[78] Liu J, Ma HL, Wei T, Liang XJ. CO_2 gas induced drug release from pH-sensitive liposome to circumvent doxorubicin resistant cells. Chem Commun (Camb) 2012;48(40):4869–71.
[79] Chung MF, Liu HY, Lin KJ, Chia WT, Sung HW. A pH-responsive carrier system that generates No bubbles to trigger drug release and reverse P-glycoprotein-mediated multidrug resistance. Angew Chem Int Ed Engl 2015;54(34):9890–3.
[80] F Quinn J, Whittaker M, Davis T. Glutathione responsive polymers and their application in drug delivery systems. Polym Chem 2016(1):97–126 ASAP.
[81] Kuppusamy P, Li H, Ilangovan G, Cardounel AJ, Zweier JL, Yamada K, et al. Noninvasive imaging of tumor redox status and its modification by tissue glutathione levels. Cancer Res 2002;62(1):307–12.
[82] Perry RR, Mazetta J, Levin M, Barranco SC. Glutathione levels and variability in breast tumors and normal tissue. Cancer 1993;72(3):783–7.
[83] Cheng R, Feng F, Meng FH, Deng C, Feijen J, Zhong ZY. Glutathione-responsive nano-vehicles as a promising platform for targeted intracellular drug and gene delivery. J Control Release 2011;152(1):2–12.
[84] Wu J, Zhao LL, Xu XD, Bertrand N, Choi WI, Yameen B, et al. Hydrophobic cysteine poly(disulfide)-based redox-hypersensitive nanoparticle platform for cancer theranostics. Angew Chem Int Ed Engl 2015;54(32):9218–23.
[85] Zhang SW, Guan JB, Sun MC, Zhang D, Zhang HT, Sun BJ, et al. Self-delivering prodrug-nanoassemblies fabricated by disulfide bond bridged oleate prodrug of docetaxel for breast cancer therapy. Drug Deliv 2017;24(1):1460–9.
[86] Bulmus V, Woodward M, Lin L, Murthy N, Stayton P, Hoffman A. A new pH-responsive and glutathione-reactive, endosomal membrane-disruptive polymeric carrier for intracellular delivery of biomolecular drugs. J Control Release 2003;93(2):105–20.
[87] Li SY, Zhang T, Xu WG, Ding JX, Yin F, Xu J, et al. Sarcoma-targeting peptide-decorated polypeptide nanogel intracellularly delivers shikonin for upregulated osteosarcoma necroptosis and diminished pulmonary metastasis. Theranostics 2018;8(5):1361–75.
[88] Ling X, Chen X, Riddell IA, Tao W, Wang JQ, Hollett G, et al. Glutathione-scavenging poly(disulfide amide) nanoparticles for effective delivery of Pt(IV) prodrugs and reversal of cisplatin resistance. Nano Lett 2018;18(7):4618–25.
[89] Tu YF, Peng F, White PB, Wilson DA. Redox-sensitive stomatocyte nanomotors: destruction and drug release in the presence of glutathione. Angew Chem Int Ed Engl 2017;56(26):7620–4.
[90] Du X, Xiong L, Dai S, Qiao SZ. Gamma-PGA-coated mesoporous silica nanoparticles with covalently attached prodrugs for enhanced cellular uptake and intracellular GSH-responsive release. Adv Healthc Mater 2015;4(5):771–81.
[91] Sun BJ, Luo C, Yu H, Zhang XB, Chen Q, Yang WQ, et al. Disulfide bond-driven oxidation- and reduction-responsive prodrug nanoassemblies for cancer therapy. Nano Lett 2018;18(6):3643–50.

[92] Zhang HC, Wang KL, Na KX, Li D, Li ZB, Zhao DY, et al. Striking a balance between carbonate/carbamate linkage bond- and reduction-sensitive disulfide bond-bearing linker for tailored controlled release: in situ covalent-albumin-binding gemcitabine prodrugs promote bioavailability and tumor accumulation. J Med Chem 2018;61(11):4904–17.
[93] Cao W, Wang L, Xu HP. Selenium/tellurium containing polymer materials in nanobiotechnology. Nano Today 2015;10(6):717–36.
[94] Cao W, Wang L, Xu HP. Coordination responsive tellurium-containing multilayer film for controlled delivery. Chem Commun (Camb) 2015;51(25):5520–2.
[95] Wang YY, Zhu LN, Wang Y, Li LB, Lu YF, Shen LQ, et al. Ultra-sensitive GSH-responsive ditelluride-containing poly(ether-urethane) nanoparticles for controlled drug release. ACS Appl Mater Interfaces 2016;8(51):35106–13.
[96] Xu HP, Cao W, Zhang X. Selenium-containing polymers: promising biomaterials for controlled release and enzyme mimics. Acc Chem Res 2013;46(7):1647–58.
[97] Shao D, Li MQ, Wang Z, Zheng X, Lao YH, Chang ZM, et al. Bioinspired diselenide-bridged mesoporous silica nanoparticles for dual-responsive protein delivery. Adv Mater 2018;30(29):e1801198.
[98] Baldwin AD, Kiick KL. Reversible maleimide-thiol adducts yield glutathione-sensitive poly(ethylene glycol)-heparin hydrogels. Polym Chem 2013;4(1):133–43.
[99] Liang YK, Kiick KL. Liposome-cross-linked hybrid hydrogels for glutathione-triggered delivery of multiple cargo molecules. Biomacromolecules 2016;17(2):601–14.
[100] Li M, Zhao LW, Zhang T, Shu Y, He ZG, Ma Y, et al. Redox-sensitive prodrug nanoassemblies based on linoleic acid-modified docetaxel to resist breast cancers. Acta Pharmaceutica Sinica B 2019;9(2):421–32.
[101] Luo C, Sun J, Liu D, Sun BJ, Miao L, Musetti S, et al. Self-assembled redox dual-responsive prodrug-nanosystem formed by single thioether-bridged paclitaxel-fatty acid conjugate for cancer chemotherapy. Nano Lett 2016;16(9):5401.
[102] Cao W, Li Y, Sun ZW, Xu HP. Coordination-responsive selenium-containing polymer micelles for controlled drug release. J Controlled Release 2012;3(12):3403–8.
[103] Cao W, Gu YW, Meineck M, Li TY, Xu HP. Tellurium-containing polymer micelles: competitive-ligand-regulated coordination responsive systems. J Am Chem Soc 2014;136(13):5132–7.
[104] Sun BJ, Luo C, Zhang XB, Guo MR, Sun MC, Yu H, et al. Probing the impact of sulfur/selenium/carbon linkages on prodrug nanoassemblies for cancer therapy. Nat Commun 2019;10(1):3211.
[105] Wang XY, Cai XP, Hu JJ, Shao NM, Wang F, Zhang Q, et al. Glutathione-triggered "off-on" release of anticancer drugs from dendrimer-encapsulated gold nanoparticles. J Am Chem Soc 2013;135(26):9805–10.
[106] Hu B, Zhao Y, Zhu HZ, Yu SH. Selective chromogenic detection of thiol-containing biomolecules using carbonaceous nanospheres loaded with silver nanoparticles as carrier. ACS Nano 2011;5(4):3166–71.
[107] Wu MY, Meng QS, Chen Y, Zhang LX, Li ML, Cai XJ, et al. Large pore-sized hollow mesoporous organosilica for redox-responsive gene delivery and synergistic cancer chemotherapy. Adv Mater 2016;28(10):1963–9.
[108] Mao HL, Xie YD, Ju HC, Mao HS, Zhao L, Wang Z, et al. Design of tumor microenvironment-responsive drug-drug micelle for cancer radiochemotherapy. ACS Appl Mater Interfaces 2018;10(40):33923–35.
[109] D'Autreaux B, Toledano MB. ROS as signalling molecules: mechanisms that generate specificity in ROS homeostasis. Nat Rev Mol Cell Biol 2007;8(10):813–24.
[110] Pelicano H, Carney D, Huang P. ROS stress in cancer cells and therapeutic implications. Drug Resist Updat 2004;7(2):97–110.
[111] Mantovani A, Allavena P, Sica A, Balkwill F. Cancer-related inflammation. Nature 2008;454(7203):436–44.
[112] Reuter S, Gupta SC, Chaturvedi MM, Aggarwal BB. Oxidative stress, inflammation, and cancer: how are they linked? Free Radic Biol Med 2010;49(11):1603–16.
[113] Newsholme P, Haber EP, Hirabara SM, Rebelato EL, Procopio J, Morgan D, et al. Diabetes associated cell stress and dysfunction: role of mitochondrial and non-mitochondrial ros production and activity. J Physiol 2010;583(1):9–24.
[114] Angelova PR, Abramov AY. Role of mitochondrial ROS in the brain: from physiology to neurodegeneration. FEBS Lett 2018;592(5):692–702.
[115] de Gracia Lux C, Joshi-Barr S, Nguyen T, Mahmoud E, Schopf E, Fomina N, et al. Biocompatible polymeric nanoparticles degrade and release cargo in response to biologically relevant levels of hydrogen peroxide. J Am Chem Soc 2012;134(38):15758–64.
[116] Yang B, Wang KY, Zhang D, Ji B, Zhao DY, Wang X, et al. Polydopamine-modified ROS-responsive prodrug nanoplatform with enhanced stability for precise treatment of breast cancer. RSC Adv 2019;9(16):9260–9.
[117] Poole KM, Nelson CE, Joshi RV, Martin JR, Gupta MK, Haws SC, et al. ROS-responsive microspheres for on demand antioxidant therapy in a model of diabetic peripheral arterial disease. Biomaterials 2015;41:166–75.
[118] Wang L, Fan FQ, Cao W, Xu HP. Ultrasensitive ROS-responsive coassemblies of tellurium-containing molecules and phospholipids. ACS Appl Mater Interfaces 2015;7(29):16054.
[119] Deepagan VG, Kwon S, You DG, Nguyen VQ, Um W, Ko H, et al. In situ diselenide-crosslinked polymeric micelles for ROS-mediated anticancer drug delivery. Biomaterials 2016;103:56–66.
[120] Deng HZ, Zhao XF, Deng LD, Liu JF, Dong AJ. Reactive oxygen species activated nanoparticles with tumor acidity internalization for precise anticancer therapy. J Control Release 2017;255:142–53.
[121] Yang B, Wang KY, Zhang D, Sun BJ, Ji B, Wei L, et al. Light-activatable dual-source ROS-responsive prodrug nanoplatform for synergistic chemo-photodynamic therapy. Biomater Sci 2018;6(11):2965–75.
[122] Jager E, Hocherl A, Janouskova O, Jager A, Hruby M, Konefal R, et al. Fluorescent boronate-based polymer nanoparticles with reactive oxygen species (ROS)-triggered cargo release for drug-delivery applications. Nanoscale 2016;8(13):6958–63.
[123] Wang M, Sun S, Neufeld CI, Perez-Ramirez B, Xu QB. Reactive oxygen species-responsive protein modification and its intracellular delivery for targeted cancer therapy. Angew Chem Int Ed Engl 2015;53(49):13444–8.
[124] Kim JS, Jo SD, Seah GL, Kim I, Nam YS. ROS-induced biodegradable polythioketal nanoparticles for intracellular delivery of anti-cancer therapeutics. J Ind Eng Chem 2015;21(1):1137–42.
[125] Xu XD, Saw PE, Tao W, Li YJ, Ji XY, Bhasin S, et al. ROS-responsive polyprodrug nanoparticles for triggered drug delivery and effective cancer therapy. Adv Mater 2017;29(33):1700141.
[126] Kankala RK, Liu CG, Chen AZ, Wang SB, Xu PY, Mende LK, et al. Overcoming multidrug resistance through the synergistic effects of hierarchical pH-sensitive,

ROS-generating nanoreactors. ACS Biomater Sci Eng 2017;3(10):2431–42.
[127] Hu JJ, Lei Q, Peng MY, Zheng DW, Chen YX, Zhang XZ. A positive feedback strategy for enhanced chemotherapy based on ROS-triggered self-accelerating drug release nanosystem. Biomaterials 2017;128:136–46 undefined.
[128] Li JJ, Ke WD, Wang L, Huang MM, Yin W, Zhang P, et al. Self-sufficing H_2O_2 -responsive nanocarriers through tumor-specific H_2O_2 production for synergistic oxidation-chemotherapy. J Control Release 2016;225:64–74.
[129] Traut TW. Physiological concentrations of purines and pyrimidines. Mol Cell Biochem 1994;140(1):1–22.
[130] Jackson RC, Lui MS, Boritzki TJ, Morris HP, Weber G. Purine and pyrimidine nucleotide patterns of normal, differentiating, and regenerating liver and of hepatomas in rats. Cancer Res 1980;40(4):1286–91.
[131] Jackson RC, Boritzki TJ, Morris HP, Weber G. Purine and pyrimidine ribonucleotide contents of rat liver and hepatoma 3924A and the effect of ischemia. Life Sci. 1976;19(10):1531–6.
[132] Sun WJ, Gu Z. ATP-responsive drug delivery systems. Expert Opin Drug Deliv 2016;13(3):311–14.
[133] Yan JH, Xiong HJ, Cai SD, Wen NC, He QY, Liu YF, et al. Advances in aptamer screening technologies. Talanta 2019;200:124–44.
[134] Liu ZB, Chen SS, Liu BW, Wu JP, Zhou YB, He LY, et al. Intracellular detection of ATP using an aptamer beacon covalently linked to graphene oxide resisting nonspecific probe displacement. Anal Chem 2014;86(24):12229–35.
[135] Wang GH, Huang GL, Zhao Y, Pu XX, Li T, Deng JJ, et al. ATP triggered drug release and dna co-delivery systems based on ATP responsive aptamers and polyethylenimine complexes. J Mater Chem B 2016;4(21):3832–41.
[136] Zhang JX, Wang YD, Chen JW, Liang X, Han HB, Yang Y, et al. Inhibition of cell proliferation through an ATP-responsive co-delivery system of doxorubicin and Bcl-2 siRNA. Int J Nanomed 2017;12:4721–32.
[137] He XX, Zhao YX, He DG, Wang MK, Xu FZ, Tang JL. ATP-responsive controlled release system using aptamer-functionalized mesoporous silica nanoparticles. Langmuir 2012;28(35):12909–15.
[138] Chen WH, Liao WC, Sohn YS, Fadeev M, Cecconello A, Nechushtai R, et al. Stimuli-responsive nucleic acid-based polyacrylamide hydrogel-coated metal-organic framework nanoparticles for controlled drug release. Adv Funct Mater 2017;28(8):1870053.
[139] Mo R, Jiang TY, DiSanto R, Tai WY, Gu Z. ATP-triggered anticancer drug delivery. Nat Commun 2014;5:3364.
[140] Mo R, Jiang TY, Gu Z. Enhanced anticancer efficacy by ATP-mediated liposomal drug delivery. Angew Chem Int Ed Engl 2014;53(23):5815–20.
[141] Mo R, Jiang TY, Sun WJ, Gu Z. ATP-responsive DNA-graphene hybrid nanoaggregates for anticancer drug delivery. Biomaterials 2015;50:67–74.
[142] Li BL, Setyawati MI, Chen LY, Xie JP, Ariga K, Lim CT, et al. Directing assembly and disassembly of 2D MoS_2 nanosheets with DNA for drug delivery. ACS Appl Mater Interfaces 2017;9(18):15286–96.
[143] Liao WC, Lu CH, Hartmann R, Wang FA, Sohn YS, Parak WJ, et al. Adenosine triphosphate-triggered release of macromolecular and nanoparticle loads from aptamer/DNA-cross-linked microcapsules. ACS Nano 2015;9(9):9078–86.
[144] Liao WC, Sohn YS, Riutin M, Cecconello A, Parak WJ, Nechushtai R, et al. The application of stimuli-responsive VEGF- and ATP-aptamer-based microcapsules for the controlled release of an anticancer drug, and the selective targeted cytotoxicity toward cancer cells. Adv Funct Mater 2016;26(24):4262–73.
[145] Liao WC, Lilienthal S, Kahn JS, Riutin M, Sohn YS, Nechushtai R, et al. pH- and ligand-induced release of loads from DNA–acrylamide hydrogel microcapsules. Chem Sci 2017;8(5):3362–73.
[146] Mo R, Jiang TY, Sun WJ, Gu Z. ATP-Responsive DNA-Graphene hybrid nanoaggregates for anticancer drug delivery. Biomaterials 2015;50(1):67–74.
[147] Fabbri F, Rotunno E, Cinquanta E, Campi D, Bonnini E, Kaplan D, et al. Novel near-infrared emission from crystal defects in MoS_2 multilayer flakes. Nat Commun 2016;7:13044.
[148] Zhou ZW, Zhang QY, Zhang MH, Li HP, Chen G, Qian CG, et al. ATP-activated decrosslinking and charge-reversal vectors for siRNA delivery and cancer therapy. Theranostics 2018;8(17):4604–19.
[149] Qian CG, Chen YL, Zhu S, Yu JC, Zhang L, Feng PJ, et al. ATP-responsive and near-infrared-emissive nanocarriers for anticancer drug delivery and real-time imaging. Theranostics 2016;6(7):1053–64.
[150] Zhou ZW, Li CZ, Zhang MH, Zhang QY, Qian CG, Oupicky D, et al. Charge and assembly reversible micelles fueled by intracellular ATP for improved siRNA transfection. ACS Appl Mater Interfaces 2018;10(38):32026–37.
[151] Naito M, Ishii T, Matsumoto A, Miyata K, Miyahara Y, Kataoka K. A phenylboronate-functionalized polyion complex micelle for ATP-triggered release of siRNA. Angew Chem Int Ed Engl 2012;51(43):10904.
[152] Kim J, Lee YM, Kim H, Park D, Kim J, Kim WJ. Phenylboronic acid-sugar grafted polymer architecture as a dual stimuli-responsive gene carrier for targeted anti-angiogenic tumor therapy. Biomaterials 2016;75:102–11.
[153] Deshayes S, Cabral H, Ishii T, Miura Y, Kobayashi S, Yamashita T, et al. Phenylboronic acid-installed polymeric micelles for targeting sialylated epitopes in solid tumors. J Am Chem Soc 2013;135(41):15501–7.
[154] Matsumoto A, Yoshida R, Kataoka K. Glucose-responsive polymer gel bearing phenylborate derivative as a glucose-sensing moiety operating at the physiological pH. Biomacromolecules 2004;5(3):1038–45.
[155] Biswas S, Kinbara K, Niwa T, Taguchi H, Ishii N, Watanabe S, et al. Biomolecular robotics for chemomechanically driven guest delivery fuelled by intracellular ATP. Nat Chem 2013;5(7):613–20.
[156] Yan Q, Zhao Y. ATP-triggered biomimetic deformations of bioinspired receptor-containing polymer assemblies. Chem Sci 2015;6(7):4343–9.
[157] Lai JP, Shah BP, Zhang YX, Yang LT, Lee KB. Real-time monitoring of ATP-responsive drug release using mesoporous-silica-coated multicolor upconversion nanoparticles. ACS Nano 2015;9(5):5234–45.
[158] Plebani M, Herszenyi L, Cardin R, Roveroni G, Carraro P, Paoli MD, et al. Cysteine and serine proteases in gastric cancer. Cancer 1995;76(3):367–75.
[159] Foekens JA, Kos J, Peters HA, Krasovec M, Look MP, Cimerman N, et al. Prognostic significance of cathepsins B and L in primary human breast cancer. J Clin Oncol 1998;16(3):1013–21.
[160] Gawenda J, Traub F, Lück HJ, Kreipe H, von Wasielewski R. Legumain expression as a prognostic factor in breast cancer patients. Breast Cancer Res Treat 2007;102(1):1–6.
[161] Herszenyi L, Farinati F, Plebani M, Istvan G, Sapi Z, Carraro P, et al. The role of cathepsins and the plasminogen activator/inhibitor system in colorectal cancer. Orv Hetil 1999;140(33):1833–6.
[162] Murthy RV, Arbman G, Gao JF, Roodman GD, Sun XF. Legumain expression in relation to clinicopathologic and

biological variables in colorectal cancer. Clin Cancer Res 2005;11(6):2293–9.
[163] Stern R. Hyaluronidases in cancer biology. Semin Cancer Biol 2008;18(4):275–80.
[164] McAtee CO, Barycki JJ, Simpson MA. Emerging roles for hyaluronidase in cancer metastasis and therapy. Adv Cancer Res 2014;123:1–34.
[165] Scomparin A, Florindo HF, Tiram G, Ferguson EL, Satchi-Fainaro R. Two-step polymer- and liposome-enzyme prodrug therapies for cancer: PDEPT and PELT concepts and future perspectives. Adv Drug Deliv Rev 2017;118:52–64.
[166] Lin S, Li T, Xie PL, Li Q, Wang BL, Wang L, et al. Targeted delivery of doxorubicin to tumour tissues by a novel legumain sensitive polygonal nanogel. Nanoscale 2016;8(43):18400–11.
[167] Zhou HC, Sun HJ, Lv SX, Zhang DW, Zhang XF, Tang ZH, et al. Legumain-cleavable 4-arm poly(ethylene glycol)-doxorubicin conjugate for tumor specific delivery and release. Acta Biomater 2017;54:227–38.
[168] He XY, Cao HQ, Wang H, Tan T, Yu HJ, Zhang PC, et al. Inflammatory monocytes loading protease-sensitive nanoparticles enable lung metastasis targeting and intelligent drug release for anti-metastasis therapy. Nano Lett 2017;17(9):5546–54.
[169] Cao HQ, Wang H, He XY, Tan T, Hu HY, Wang ZW, et al. Bioengineered macrophages can responsively transform into nanovesicles to target lung metastasis. Nano Lett 2018;18(8):4762–70.
[170] Huang HT, Geng JQ, Golzarian J, Huang J, Yu JH. Fabrication of doxorubicin-loaded ellipsoid micelle based on diblock copolymer with a linkage of enzyme-cleavable peptide. Colloids Surf B Biointerfaces 2015;133:362–9.
[171] Han HJ, Valdeperez D, Jin Q, Yang B, Li ZH, Wu YL, et al. Dual enzymatic reaction-assisted gemcitabine delivery systems for programmed pancreatic cancer therapy. ACS Nano 2017;11(2):1281–91.
[172] Cheng YJ, Luo GF, Zhu JY, Xu XD, Zeng X, Cheng DB, et al. Enzyme-induced and tumor-targeted drug delivery system based on multifunctional mesoporous silica nanoparticles. ACS Appl Mater Interfaces 2015;7(17):9078–87.
[173] Shim MK, Park J, Yoon HY, Lee S, Um W, Kim JH, et al. Carrier-free nanoparticles of cathepsin B-cleavable peptide-conjugated doxorubicin prodrug for cancer targeting therapy. J Control Release 2019;294:376–89.
[174] Giusti I, D'Ascenzo S, Millimaggi D, Taraboletti G, Carta G, Franceschini N, et al. Cathepsin B mediates the pH-dependent proinvasive activity of tumor-shed microvesicles. Neoplasia 2008;10(5):481–8.
[175] Lee JS, Groothuis T, Cusan C, Mink D, Feijen J. Lysosomally cleavable peptide-containing polymersomes modified with anti-EGFR antibody for systemic cancer chemotherapy. Biomaterials 2011;32(34):9144–53.
[176] Shim MK, Yoon HY, Ryu JH, Koo H, Lee S, Park JH, et al. Cathepsin B-specific metabolic precursor for in vivo tumor-specific fluorescence imaging. Angew Chem Int Ed Engl 2016;55(47):14698–703.
[177] Bernardos A, Mondragon L, Aznar E, Marcos MD, Martinez-Manez R, Sancenon F, et al. Enzyme-responsive intracellular controlled release using nanometric silica mesoporous supports capped with "saccharides". ACS Nano 2010;4(11):6353–68.
[178] Mondragon L, Mas N, Ferragud V, de la Torre C, Agostini A, Martinez-Manez R, et al. Enzyme-responsive intracellular-controlled release using silica mesoporous nanoparticles capped with epsilon-poly-L-lysine. Chemistry 2014;20(18):5271–81.
[179] Awino JK, Gudipati S, Hartmann AK, Santiana JJ, Cairns-Gibson DF, Gomez N, et al. Nucleic acid nanocapsules for enzyme-triggered drug release. J Am Chem Soc 2017;139(18):6278–81.
[180] Murata M. Inflammation and cancer. Environ Health Prev Med 2002(6917):860–7.
[181] Nakamura K, Smyth MJ. Targeting cancer-related inflammation in the era of immunotherapy. Immunol Cell Biol 2017;95(4):325–32.
[182] Xue JW, Zhao ZK, Zhang L, Xue LJ, Shen SY, Wen YJ, et al. Neutrophil-mediated anticancer drug delivery for suppression of postoperative malignant glioma recurrence. Nat Nanotechnol 2017;12(3):692–700.
[183] Huang YK, Gao XL, Chen J. Leukocyte-derived biomimetic nanoparticulate drug delivery systems for cancer therapy. Acta Pharm Sin B 2018;8(1):4–13.
[184] Montague SJ, Andrews RK, Gardiner EE. Mechanisms of receptor shedding in platelets. Blood 2018;132(24):2535–45.
[185] Krishnamurthy S, Gnanasammandhan MK, Xie C, Huang K, Cui MY, Chan JM. Monocyte cell membrane-derived nanoghosts for targeted cancer therapy. Nanoscale 2016;8(13):6981–5.
[186] Goh WJ, Zou S, Czarny B, Pastorin G. nCVTs: a hybrid smart tumour targeting platform. Nanoscale 2018;10(15):6812–19.
[187] Cao HQ, Dan ZL, He XY, Zhang ZW, Yu HJ, Yin Q, et al. Liposomes coated with isolated macrophage membrane can target lung metastasis of breast cancer. ACS Nano 2016;10(8):7738–48.
[188] Choi J, Kim HY, Ju EJ, Jung J, Park J, Chung HK, et al. Use of macrophages to deliver therapeutic and imaging contrast agents to tumors. Biomaterials 2012;33(16):4195–203.
[189] Si JX, Shao SQ, Shen YQ, Wang K. Macrophages as active nanocarriers for targeted early and adjuvant cancer chemotherapy. Small 2016;12(37):5108–19.
[190] Fesnak AD, June CH, Levine BL. Engineered T cells: the promise and challenges of cancer immunotherapy. Nat Rev Cancer 2016;16(9):566–81.
[191] Huang B, Abraham WD, Zheng Y, Bustamante Lopez SC, Luo SS, Irvine DJ. Active targeting of chemotherapy to disseminated tumors using nanoparticle-carrying T cells. Sci Transl Med 2015;7(291):291ra94.
[192] Steinfeld U, Pauli C, Kaltz N, Bergemann C, Lee HH. T lymphocytes as potential therapeutic drug carrier for cancer treatment. Int J Pharm 2006;311(1):229–36.
[193] Stephan MT, Moon JJ, Um SH, Bershteyn A, Irvine DJ. Therapeutic cell engineering with surface-conjugated synthetic nanoparticles. Nat Med 2010;16(9):1035–41.
[194] Tsou P, Katayama H, Ostrin EJ, Hanash SM. The emerging role of B cells in tumor immunity. Cancer Res 2016;76(19):5597–601.
[195] Hu QY, Sun WJ, Qian CG, Wang C, Bomba H, Gu Z. Anticancer platelet-mimicking nanovehicles. Adv Mater 2016;27(44):7043–50.
[196] Wang C, Sun WJ, Ye YQ, Hu QY, Bomba HN, Gu Z. In situ activation of platelets with checkpoint inhibitors for post-surgical cancer immunotherapy. Nat Biomed Eng 2017;1(2):0011.
[197] Pang L, Zhang C, Qin J, Han LM, Li RX, Hong C, et al. A novel strategy to achieve effective drug delivery: exploit cells as carrier combined with nanoparticles. Drug Deliv 2017;24(1):83–91.
[198] Timin AS, Litvak MM, Gorin DA, Atochina-Vasserman EN, Atochin DN, Sukhorukov GB. Cell-based drug delivery and use of nano-and microcarriers for cell functionalization. Adv Healthc Mater 2018;7(3):1700818.
[199] Hu QY, Sun WJ, Wang JQ, Ruan HT, Zhang XD, Ye YQ, et al. Conjugation of haematopoietic stem cells and

platelets decorated with anti-PD-1 antibodies augments anti-leukaemia efficacy. Nat Biomed Eng 2018;2(11):831–40.
[200] Kim J, Jo C, Lim WG, Jung S, Lee YM, Lim J, et al. Programmed nanoparticle-loaded nanoparticles for deep-penetrating 3D cancer therapy. Adv Mater 2018:e1707557.
[201] Zhang PH, Wang Y, Lian J, Shen Q, Wang C, Ma BH, et al. Engineering the surface of smart nanocarriers using a pH-/thermal-/GSH-responsive polymer zipper for precise tumor targeting therapy *in vivo*. Adv Mater 2017;29(36):1702311.
[202] Wang QL, Zhang P, Li ZM, Feng XR, Lv CY, Zhang HY, et al. Evaluation of polymer nanoformulations in hepatoma therapy by established rodent models. Theranostics 2019;9(5):1426–52.
[203] Hanlon DJ, Aldo PB, Devine L, Alvero AB, Engberg AK, Edelson R, et al. Enhanced stimulation of anti-ovarian cancer CD8+ T cells by dendritic cells loaded with nanoparticle encapsulated tumor antigen. Am J Reprod Immunol 2011;65(6):597–609.
[204] Stubbs M, McSheehy PMJ, Griffiths JR. Causes and consequences of acidic pH in tumors: a magnetic resonance study. Advances in Enzyme Regulation 1999;39(1):13–30.
[205] Perry RR, Mazetta J, Levin M, Barranco SC. Glutathione levels and variability in breast tumors and normal tissue. Cancer 1993;72(3):783–7.
[206] Montero D, Tachibana C, Rahr Winther J, Appenzeller-Herzog C. Intracellular glutathione pools are heterogeneously concentrated. Redox Biology 2013;1(1):508–13.
[207] Arian D, Kovbasyuk D, Mokhir A. 1,9-Dialkoxyanthracene as a $^{1}O2$-sensitive linker. J Am Chem Soc 2011;133(11):3972–80.
[208] Gribble FM, Loussouarn G, Tucker SJ, Zhao C, Nichols CG, Ashcroft FM. A novel method for measurement of submembrane ATP concentration. J Biol Chem 2000;275(39):30046–9.
[209] Leist M, Single B, Castoldi AF, Kuhnle S, Nicotera P. Intracellular adenosine triphosphate (ATP) concentration: a switch in the decision between apoptosis and necrosis. J Exp Med 1997;185(8):1481–6.
[210] Gorman MW, Feigl EO, Castoldi AF, Buffington CW. Human plasma ATP concentration. Clin. Chem. 2007;53(2):318–25.